

Article

# Analysis of Parameters of a Rectified Tank on the Basis of In-Situ Tests

Krzysztof Gromysz 

Department of Building Structures, Faculty of Civil Engineering, Silesian University of Technology,  
44-100 Gliwice, Poland; krzysztof.gromysz@polsl.pl

**Abstract:** The vertical deflection of building structures is a common problem. However, the rectification of objects is rarely carried out due to the lack of information about the parameters of objects requiring rectification. The subject of the analysis are parameters of rectified water tank 950 m<sup>3</sup> in volume, which were investigated due to the stiffness and number of supports built into the structure. During in-situ testing, the stiffnesses of supports were determined. The model of the rectified structure was then defined and it was shown that its parameters can be described by means of three matrices: stiffness, displacement forms of the elevated object and displacement forms of supports. Absolute values of elements of the stiffness matrix increased as the stiffness and number of supports increased. At the same time, values of elements of the matrix of displacement forms of the elevated object increased. The conducted energy analysis demonstrated that the amount of energy required for the vertical displacement of the structure decreased with an increasing stiffness and number of supports. This means that placing a greater number of supports under rectified structures and ensuring more rigid supports is beneficial to the rectification. Results of the conducted analyses were confirmed during in-situ tests.

**Keywords:** support stiffness; parameters of the structure; stiffness matrix; form of displacement; vertical deflection of building structure; rectification; work done on moving building objects



**Citation:** Gromysz, K. Analysis of Parameters of a Rectified Tank on the Basis of In-Situ Tests. *Materials* **2021**, *14*, 3881. <https://doi.org/10.3390/ma14143881>

Academic Editor:  
Francesco Fabbrocino

Received: 17 June 2021  
Accepted: 8 July 2021  
Published: 12 July 2021

**Publisher's Note:** MDPI stays neutral with regard to jurisdictional claims in published maps and institutional affiliations.



**Copyright:** © 2021 by the author. Licensee MDPI, Basel, Switzerland. This article is an open access article distributed under the terms and conditions of the Creative Commons Attribution (CC BY) license (<https://creativecommons.org/licenses/by/4.0/>).

## 1. Introduction

Vertical deflection is a common defect of building structures. This effect is mainly caused by insufficient load-bearing capacity of subsoil [1,2]. This problem concerns different types of construction: grain elevators [3], historic masonry [4] and wood towers [5,6], churches [7], and residential buildings [8]. Deflection of building objects can be also caused by earthquakes [9], wind loading [10] and the construction of tunnels in their vicinity [11]. Moreover, many buildings are deflected as the effect of non-uniform subsidence of mining areas [12], resulting from the compression of voids left after coal bed extraction [13]. Subsidence of the mining area may take the form of continuous [14,15] or discontinuous deformation [16]. Deflections can be also caused by exploitation of groundwater reservoirs [17]. However, deflection increases the seismic vulnerability of towers [18], slender structures and tall buildings [19]. Moreover, deflection, an effect of nonuniform settlement of the ground, can damage constructions with wall building structure [20,21], frame structures [22], foundations [23] which can increase the risk of building operation [24], and the risk of collapse [25]. Deflected structures are usually stabilized by reinforcing their foundation with steel [26] or reinforced concrete piles [27], or by reinforcing the ground [4]. In case of the deflection of single elements of the structure, they are stabilised in a new position [28]. In particular situations, structural elements [29] or whole buildings [30] are rectified. This method can be based on removing soil from parts of the building that are too high [31–33] or elevating parts of the building that are too low [34] through the use of temporary supports [35]. The previous tests included the rectification of buildings which were divided into two parts, one of them remaining in the ground, while the other was non-uniformly elevated. Such a process with reference to historic two-storey building is

described in [36]. No tests have been performed so far on parameters of rectified structures that are elevated in a non-uniform way with the foundation slab.

Hence, this paper defines a model of structure elevated in a non-uniform way with the foundation slab. Model parameters are determined for fire fighting storage tank of 950 m<sup>3</sup> in volume. This structure was built on human-altered soil which caused its deflection.

The steel tank has a cylindrical shape with an inner diameter of 12.221 m and a height of 8.520 m (Figure 1). Its shell is made of a metal sheet of 3 mm in thickness and reinforced with elements made of an angle section placed at four levels. The roof structure is composed of steel beams made of cold-formed steel elements supported on the reinforced edge of the shell and two columns placed inside the tank. A three-layer panel with polyurethane core is used as the roofing material. Inside the tank, there are water supply systems and components of the fire-fighting system used to pump out water. Waterproofing is ensured by PVC film of 1.5 mm in thickness which is placed inside the tank.

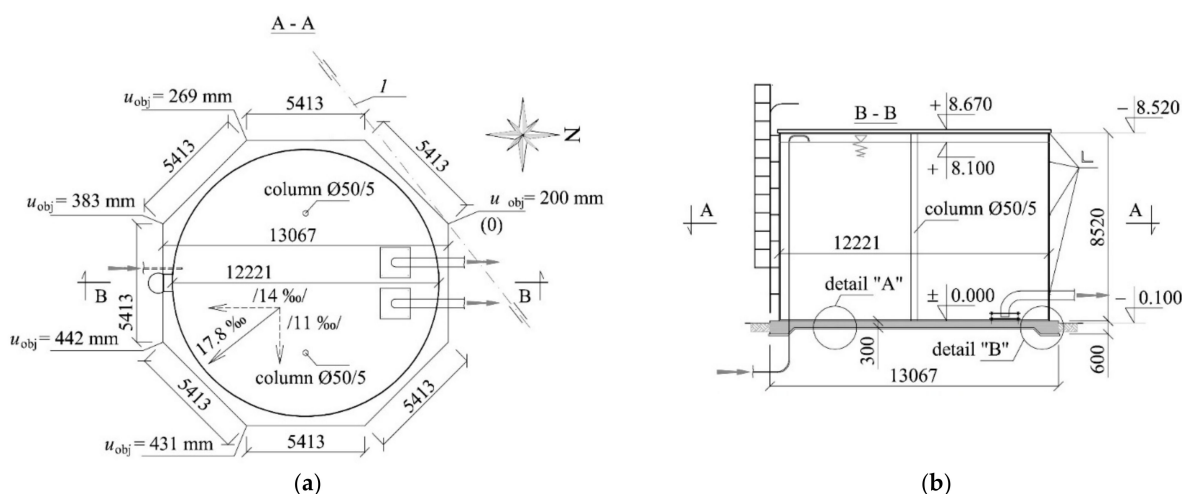


**Figure 1.** Tested steel water tank placed on the reinforced concrete foundation slab: (a) tank plan; (b) cross-section, 1—centre of rotation during rectification, 17.8‰—resultant deflection, /14‰/, /11‰/—components of deflection.

The tank is placed on a reinforced concrete foundation slab of octagonal shape and a side length equal to 5.413 m. The slab has a thickness of 300 mm (Figure 2a). However, the thickness changes gently at the edges up to 600 mm and the reinforced concrete beam formed around the slab has a cross-section of (b/h) 800 mm/600 mm (Figure 2b). A layer of lean concrete of 70 mm in thickness is placed under the slab. The 2-way reinforcement of upper and bottom slabs is composed of rebars of 12 mm in diameter and the spacing of 150 mm. The bottom reinforcement of the beam around the slab contains six rebars having a diameter of 16 mm and stirrups made of bars of 8 mm in diameter with the spacing of 250 mm. The weight of an empty tank with the foundation slab is 1347 kN.

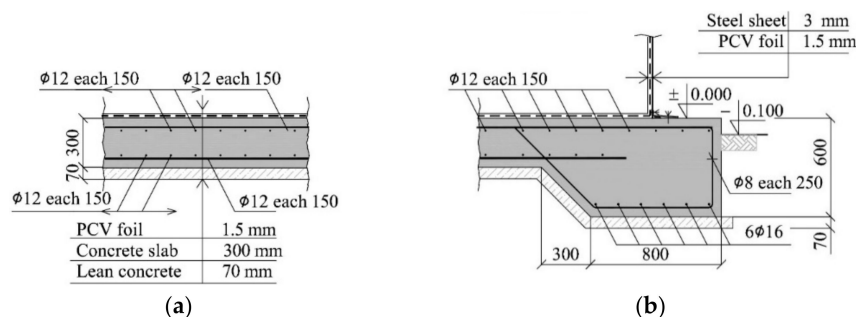


**Figure 2.** Reinforced concrete foundation slab of the tank: (a) detail “A” from Figure 1; (b) detail “B” from Figure 1.

The tank was deflected by 17.8 mm/m from vertical in the south-east direction. Consequently, it required the rectification. For that purpose 16 stacks of concrete blocks were pressed into the ground under reinforced concrete slab. Then, 16 hydraulic jacks were placed on these jack supports. These jacks took the weight of the tank. They were used to elevate uniformly the tank and the foundation by 200 mm, and then the rectification began by non-uniform elevation. It means the whole tank was rotated around axis 1 (Figure 1). The minimum elevation  $u_{obj}$  was 200 mm, and the maximum 431 mm (Figure 1). Space between the slab base and the ground formed as the result of rectification was filled with concrete.

In-situ testing of the structure placed on the hydraulic jacks was performed before and after the rectification. The results were used to determine stiffness of jack and jack supports and to determine the parameters of the rectified tank.

It should be noted that no tests have been performed so far on parameters of tanks that are elevated with the foundation slab in a non-uniform way. Similarly, no research into the lifting of whole building objects have been undertaken in the literature.

### 2. Parameters of Rectified Tank

To define parameters of the rectified tank resting on the hydraulic jacks, the following elements were assumed to be elements of the tested system (Figure 3a): elevated tank (1), hydraulic jacks (2) and jack supports (3). Pistons (2a) and cylinders (2b) were considered to be exposed to independent extensions and deformations.

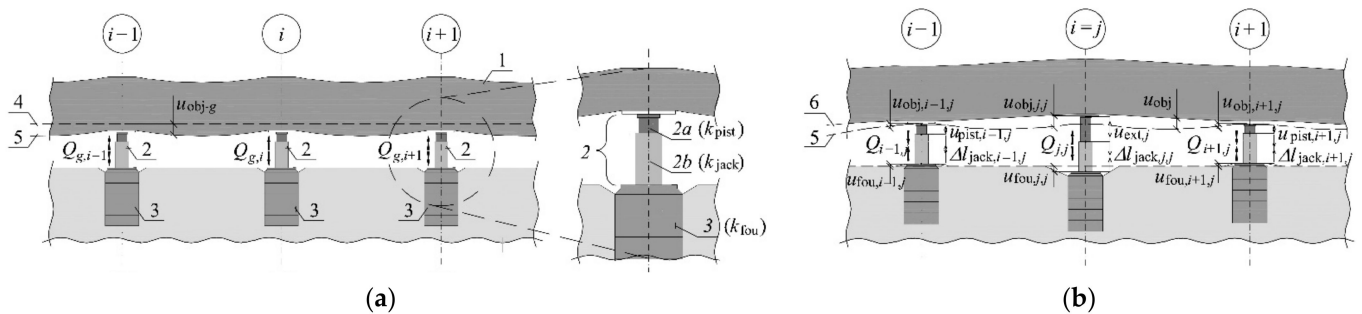


**Figure 3.** Displacements of the structure components, piston extensions and changes in forces in the jacks: (a) tank resting on the jacks prior to lifting; (b) tank after forced piston extension in the active  $j$ -th jack of value  $u_{ext,j}$ : 1—elevated tank, 2—jack (2a—piston characterized by stiffness  $k_{pist}$ , 2b—cylinder characterized by stiffness  $k_{jack}$ ), 3—jack support characterized by stiffness  $k_{fou}$ , 4—position of the tank before installing the jacks, 5—position of the tank when jacks took the tank weight, 6—position of the elevated tank after the forced piston extension by the value  $u_{ext,j}$ .

When the jacks took the tank weight, in each of them was generated the force  $Q_{g,i}$  whose value resulted from dead load and stiffness of individual components of the structure. Additionally, as the tank was placed on the jacks, it was deformed because of the acting dead load. The bottom edge of the slab changed its position of  $u_{obj-g}$  value from (4) to (5) (Figure 3a). Each  $i$ -th support for the jack was also displaced.

#### Passive and Active Jacks

Each of  $n$  jacks, on which the tank is placed, can operate as active or passive jack during lifting. The piston forced extension by the value  $u_{ext,j}$  was forced in the active  $j$ -th jack (Figure 3b). This extension resulted in the displacements  $u_{obj}$  of the structure with reference to the position  $u_{obj-g}$ , the piston extension in the adjacent jacks, displacement of jack supports, changes in the length of cylinders, and changes in values of forces in jacks.

The dual  $i, j$  indices specifying the effect of the forced piston extension in the  $j$ -th jack were assumed. The index  $i$  means a point number of the structure and the jack number, that effects are specified for the position of its installation. The index  $j$  corresponds to the number of the active jack, whose piston extension is forced. Each jack can be active or passive. Thus, the indices  $i$  and  $j$  can take values  $1, 2, \dots, n$ , where  $n$  is the number of jacks

installed under the tank. When the index specifying a given value is  $i = j$ , then it refers to changes in the position of the jack which is active at that moment.

Value  $u_{\text{ext},j}$  of the forced piston extension in the  $j$ -th active jack ( $i = j$ ) generated an increase in the force by  $Q_{j,j}$  and resulted in the following changes at the point of the installed jack (Figure 3b):

- Upward displacement of value  $u_{\text{obj},j,j}$  of the elevated structure;
- Downward displacement of value  $u_{\text{obj},j,j}$  of the jack support;
- Change  $\Delta l_{\text{jack},j,j}$  of the jack cylinder length.

The relationship between a change in the force value  $Q_{j,j}$  of the jack and the forced piston extension  $u_{\text{ext},j}$  ( $i = j$ ) was assumed to be linear

$$k_{j,j} = \frac{Q_{j,j}}{u_{\text{ext},j}}, \quad (1)$$

where  $k_{j,j}$  is the structure stiffness at the point of forced displacement  $u_{\text{ext},j}$ .

The forced piston extension in the  $j$ -th active jack changed the force in the  $i$ -th passive jack of value  $Q_{i,j}$ , caused the free piston extension  $u_{\text{pist},i,j}$  of this jack and caused the following effects at the point of the installed  $i$ -th passive jack (Figure 3b):

- Upward displacement of value  $u_{\text{obj},i,j}$  of the elevated part;
- Downward displacement of value  $u_{\text{fou},i,j}$  of the jack support;
- Change  $\Delta l_{\text{jack},i,j}$  of the jack cylinder length.

The relationship between a change in  $Q_{i,j}$  and  $u_{\text{ext},j}$  was assumed to be linear

$$k_{i,j} = \frac{Q_{i,j}}{u_{\text{ext},j}}, \quad (2)$$

where  $k_{i,j}$  is a change in the force of the  $i$ -th passive jack caused by the forced piston extension  $u_{\text{ext},j}$  equal to 1 in the  $j$ -th jack.

The jacks placed on the jack supports functioned as one-sided supports that did not transfer tensile forces. However, no pull-off was observed in these supports which was a consequence of high values  $Q_{g,i}$  resulting from the tank weight and low values  $u_{\text{ext},j}$  of the forced piston extension. Therefore, the jack support model was assumed to be an element having the constant stiffness both at increasing and decreasing force in the support. The jack support, jack cylinder and its piston had the following stiffness values  $k_{\text{fou}}$ ,  $k_{\text{jack}}$ ,  $k_{\text{pist}}$ , which were defined as

$$k_{\text{fou}} = \frac{Q_{i,j}}{u_{\text{fou},i,j}}, \quad k_{\text{jack}} = \frac{Q_{i,j}}{u_{\text{jack},i,j}}, \quad k_{\text{pist}} = \frac{Q_{i,j}}{u_{\text{pist},i,j}}. \quad (3)$$

On the basis of the linear relationship between the forced extension  $u_{\text{ext},j}$  of the piston and any displacement of the structure caused by this extension, the following constants for the structure were assumed

$$f_{\text{obj},i,j} = \frac{u_{\text{obj},i,j}}{u_{\text{ext},j}}, \quad (4)$$

$$f_{\text{fou},i,j} = \frac{u_{\text{fou},i,j}}{u_{\text{ext},j}}, \quad (5)$$

which define displacements of the elevated structure and the jack support caused by forced piston extension  $u_{\text{ext},j}$  equal to 1.2.2. Description of Rectified Tank Expressed by Matrices

Changes in values of jack forces resulting from any forced piston extension can be expressed as:

$$\mathbf{Q} = \mathbf{k}u_{\text{ext}} \quad (6)$$

where

$$Q = \begin{bmatrix} Q_1 \\ Q_2 \\ \dots \\ Q_i \\ \dots \\ Q_n \end{bmatrix}, \quad \mathbf{u}_{\text{ext}} = \begin{bmatrix} u_{\text{ext},1} \\ u_{\text{ext},2} \\ \dots \\ u_{\text{ext},j} \\ \dots \\ u_{\text{ext},n} \end{bmatrix} \quad (7)$$

are vectors of changes in jack forces and forced piston extensions, and  $\mathbf{k}$  is the stiffness matrix

$$\mathbf{k} = \begin{bmatrix} k_{1,1} & k_{1,2} & \dots & k_{1,j} & \dots & k_{1,n} \\ k_{2,1} & k_{2,2} & \dots & k_{2,j} & \dots & k_{2,n} \\ \dots & \dots & \dots & \dots & \dots & \dots \\ k_{i,1} & k_{i,2} & \dots & k_{i,j} & \dots & k_{i,n} \\ \dots & \dots & \dots & \dots & \dots & \dots \\ k_{n,1} & k_{n,2} & \dots & k_{n,j} & \dots & k_{n,n} \end{bmatrix} \quad (8)$$

of the rectified tank placed on jacks, where  $k_{j,j}$  ( $i = j$ ), calculated from (1) and  $k_{i,j}$  ( $i \neq j$ ) calculated from (2).

The forced piston extension in the  $j$ -th jack cause displacements of elevated tank and jack supports. It was assumed that those displacements are represented by two vectors denoted as vectors of displacement forms of the elevated object and of the jack supports

$$\mathbf{f}_{\text{obj},j} = \begin{bmatrix} f_{\text{obj},1,j} \\ f_{\text{obj},2,j} \\ \dots \\ f_{\text{obj},i,j} \\ \dots \\ f_{\text{obj},n,j} \end{bmatrix}, \quad \mathbf{f}_{\text{fou},j} = \begin{bmatrix} f_{\text{fou},1,j} \\ f_{\text{fou},2,j} \\ \dots \\ f_{\text{fou},i,j} \\ \dots \\ f_{\text{fou},n,j} \end{bmatrix}, \quad (9)$$

where  $f_{\text{obj},i,j}$  was calculated from (4), and  $f_{\text{fou},i,j}$  was calculated from (5). Those vectors define with accuracy to the constant factor, the distribution of displacements of the elevated object and of the jack supports. The vector  $\mathbf{f}_{\text{obj},j}$  was used to denote the  $j$ -th form of displacements of the elevated tank, and  $\mathbf{f}_{\text{fou},j}$  was the  $j$ -th form of displacements of jack supports.

A set of vectors  $\mathbf{f}_{\text{obj},j}$  formed a matrix of displacement forms of the elevated part

$$\mathbf{f}_{\text{obj}} = [ \mathbf{f}_{\text{obj},1} \quad \mathbf{f}_{\text{obj},2} \quad \dots \quad \mathbf{f}_{\text{obj},j} \quad \dots \quad \mathbf{f}_{\text{obj},n} ] \quad (10)$$

and a set of vectors  $\mathbf{f}_{\text{fou},j}$  formed a matrix of displacement forms of the jack supports

$$\mathbf{f}_{\text{fou}} = [ \mathbf{f}_{\text{fou},1} \quad \mathbf{f}_{\text{fou},2} \quad \dots \quad \mathbf{f}_{\text{fou},j} \quad \dots \quad \mathbf{f}_{\text{fou},n} ]. \quad (11)$$

Therefore the vector  $\mathbf{u}_{\text{obj}}$  of displacement of all  $n$  points of the elevated tank can be expressed as

$$\mathbf{u}_{\text{obj}} = \mathbf{f}_{\text{obj}} \mathbf{u}_{\text{ext}} \quad (12)$$

and the vector  $\mathbf{u}_{\text{fou}}$  of displacement of all  $n$  jack supports can be expressed as

$$\mathbf{u}_{\text{fou}} = \mathbf{f}_{\text{fou}} \mathbf{u}_{\text{ext}}. \quad (13)$$

The displacement vector  $\mathbf{u}_{\text{o-f}}$  for the elevated tank against the jack support was equal to

$$\mathbf{u}_{\text{o-f}} = \mathbf{u}_{\text{obj}} - \mathbf{u}_{\text{fou}} \quad (14)$$

and using the Equations (6) and (14), it can be expressed as

$$\mathbf{u}_{o-f} = (\mathbf{f}_{obj} - \mathbf{f}_{fou}) \mathbf{k}^{-1} \mathbf{Q}. \quad (15)$$

If the elements  $f_{fou,i,j}$  of the matrix  $\mathbf{f}_{fou}$  tend to zero, which corresponds to the rigid jack supports, then the displacements  $\mathbf{u}_{obj}$  can be expressed as

$$\mathbf{u}_{obj} = \mathbf{f}_{obj} \mathbf{k}^{-1} \mathbf{Q}. \quad (16)$$

The work  $W_j$  done by the active support ( $i = j$ ), in which there is the force  $Q_j$ , resulted from the work of this force acting upon the forced piston extension  $u_{ext,j}$  and deformation of the whole structure, was equal to

$$W_{jack,j} = Q_i u_{ext,j} + \frac{1}{2} k_{j,j} u_{ext,j}^2. \quad (17)$$

The force value  $Q_i$  in the  $i$ -th jack resulted from the value  $Q_{g,i}$  and the history of forced piston extensions  $u_{ext}$ . Assuming that the piston extension was forced in the jacks denoted by letters from  $r$  to  $s$ , then

$$Q_i = Q_{g,i} + \sum_{j=r}^s k_{i,j} u_{ext,j}. \quad (18)$$

Based on the Equations (17) and (18), the relationship was derived for work  $W$  done by all  $n$  jacks when the forced extension in each of them was equal  $u_{ext,j} = u_{ext}$

$$W = u_{ext} \sum_{j=1}^n Q_{g,j} + u_{ext}^2 \left( \frac{1}{2} \sum_{j=1}^n k_{j,j} + \sum_{i=2}^n \sum_{j=1}^{i-1} k_{i,j} \right). \quad (19)$$

The expression (19) is a sum of two members. The first member, where the displacement  $u_{ext}$  occurred, expresses a change in potential energy of the construction as the rigid body. The second member at the symbol  $(u_{ext})^2$  defines a change in potential energy of deformed jacks, the elevated part and the supports.

### 3. Purpose and Plan of Tests

The purpose of the tests was to determine parameters  $\mathbf{k}$ ,  $\mathbf{f}_{obj}$  and  $\mathbf{f}_{fou}$  of the rectified tank, including real stiffness of elements of the tank supports. Therefore, in-situ testing of the tank placed on  $n = 16$  jacks was performed before and after the rectification. These tests were used to determine stiffness for the support elements  $k_{jack}$ ,  $k_{pist}$ ,  $k_{fou}$ , and the stiffness  $k_{j,j}$  (Figure 4). Then, the searched parameters were determined for these stiffness values and the taken model for the rectified tank.

Moreover, the aim of these tests was to analyse the effect of the model variables, which include the  $n$  number of the jacks and the jack support stiffness  $k_{fou}$ , on the analysed parameters  $\mathbf{k}$ ,  $\mathbf{f}_{obj}$  and  $\mathbf{f}_{fou}$ . The analyses were conducted for the  $n$  number of jacks equal to 3, 4, 8, 16, 32 (Figure 4) and six different stiffness values for the jack support  $k_{fou-1}$ ,  $k_{fou-2}$ ,  $k_{fou-3}$ ,  $k_{fou-4}$ ,  $k_{fou-5}$  and  $k_{fou-6}$ . The stiffness  $k_{fou-3}$  was determined from the tests, whereas other values were freely chosen provided that  $k_{fou-1} < k_{fou-2} < k_{fou-3} < k_{fou-4} < k_{fou-5} < k_{fou-6}$ . The aim of these analyses also consisted in expressing the effect of the model variables on the work done by the jacks during the elevation of the tank.

The hydraulic piston jacks were used for the in-situ tests and the rectification process (Figure 5). The jack was composed of the elements that transmitted loads: piston (1), cylinder (2) and other items, such as: oil pump (3), solenoid valves (4), oil tank (5), control box (6) and frame (7). The jacks rested on the jack supports which were made of stacks of concrete blocks pressed under the foundation slab. The stacks were pressed when the tank was filled with water, whereas the in-situ tests and the rectification were conducted after pumping out water from the tank.

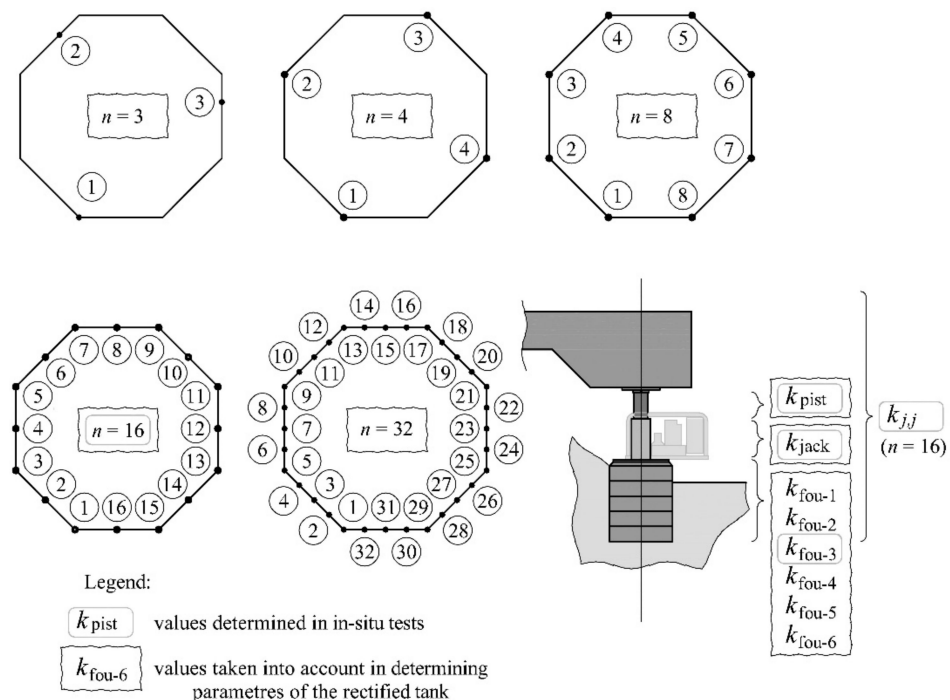


**Figure 4.** Values determined during the in-situ tests ( $k_{pist}$ ,  $k_{jack}$ ,  $k_{fou-3}$ ) and the model variables ( $n$ ,  $k_{fou}$ ), for which the parameters  $k$ ,  $f_{obj}$  and  $f_{fou}$  of the rectified tank were calculated ( $k_{fou-1} < k_{fou-2} < k_{fou-3} < k_{fou-4} < k_{fou-5} < k_{fou-6}$ ).



**Figure 5.** Hydraulic jack: (a) scheme; (b) view: 1—piston, 2—cylinder, 3—oil pump, 4—solenoid valves, 5—oil tank, 6—control box, 7—frame.

### 3.1. In-Situ Testing

The in-situ tests were planned to be performed in two stages. The following stiffness values for the support elements were determined prior to the rectification:  $k_{jack}$ ,  $k_{pist}$  and  $k_{fou}$ . For this purpose, the jacks were placed on previously prepared jack supports at points 1, 3 and 15 (Figure 6a) under the slab. The jack 1 was a passive one, while the piston extension in the jacks 3 and 15 was cyclically increasing or decreasing. Thus, a change in the force generated by the passive jack (1) was forced within the range from  $Q_{min}$  to  $Q_{max}$ . The force  $Q$  and associated displacements  $u_{fou}$ ,  $u_{pist}$  as well as a change in the length  $\Delta l_{jack}$  of the jack cylinder were measured during the tests. The force was measured by recording oil pressure in the jack. The displacements and a change in the cylinder length were measured using two linear variable differential transducers (LVDT) with an accuracy of 0.001 mm by measuring  $u_{fou(r)}$ ,  $u_{fou(l)}$  and  $u_{pist(r)}$ ,  $u_{pist(l)}$ , and also  $\Delta l_{jack(r)}$ ,  $\Delta l_{jack(l)}$  (Figure 6b). Displacements  $u_{fou(r)}$ ,  $u_{fou(l)}$  of the jack supports against the ground were measured by measuring the displacement of the top surface area of the jack support (Figure 6c) against the bars driven into the ground to a depth of 1.5 m. Other measurements were taken for relative displacements of adequate points of the structure

elements (Figure 6d). The places where the measurements were made and the measured values are shown in Figure 7a,b. The tank, while determining the parameters  $k_{i,j}$ , is shown in Figure 7c,d.

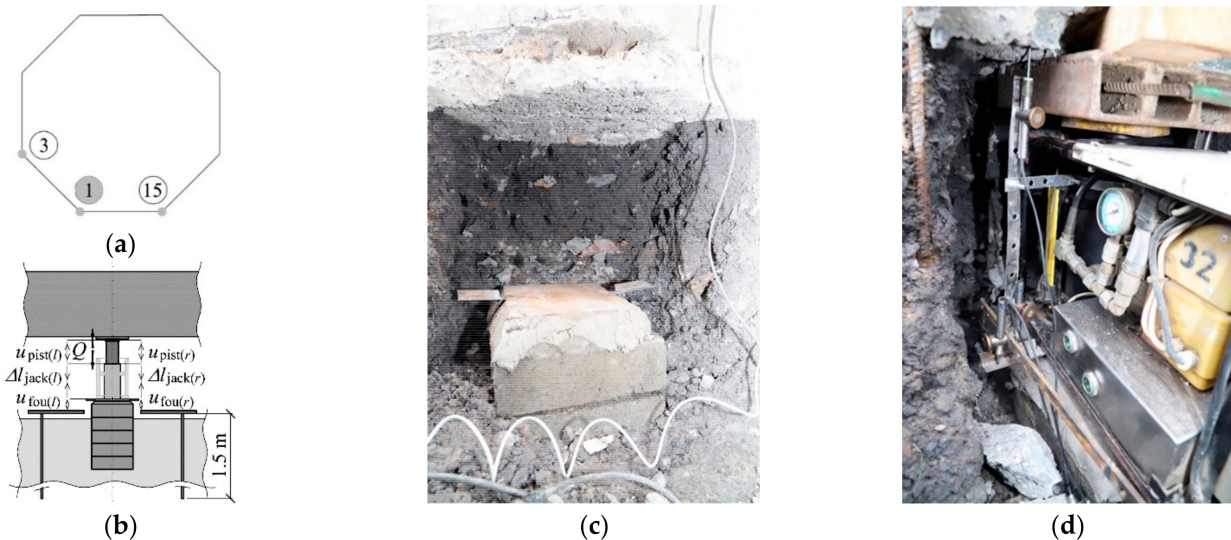


**Figure 6.** In-situ testing of stiffness  $k_{jack}$ ,  $k_{pist}$  and  $k_{fou}$ : (a) position of the installed passive jack (1) and active jacks (3, 15); (b) plan of measurements (passive jack); (c) jack support in the form of a stack of concrete blocks pressed under the foundation slab; (d) jack placed on the jack support and prepared for tests.



**Figure 7.** In-situ testing of stiffness  $k_{j,j}$  ( $j = 1, \dots, 16$ ), (a) positions of the installed jacks and points of measuring the values  $u_{ext,j}$  and  $Q_{j,j}$ ; (b) plan of measurements; (c) tank placed on  $n = 16$  jacks; (d) jack prepared for the tests, (e) space formed under the foundation slab after the rectification.

The stiffness  $k_{j,j}$  of the structure at the points  $j$  ( $j = 1, \dots, 16$ ) defined by the expression (1) were determined after the rectification. Consequently, the piston extension  $u_{ext,j}$  in the  $j$ -th jack was forced for each support and a change in the force  $Q_{j,j}$  produced by a given jack was recorded.

### 3.2. In-Situ Testing

Parameters of the tank placed on the jacks were determined from numerical calculations performed for the model of the structure. These parameters included the stiffness matrix  $\mathbf{k}$ , the matrix  $\mathbf{f}_{\text{obj}}$  of displacement forms of the elevated tank and the matrix  $\mathbf{f}_{\text{fou}}$  of displacement forms of jack supports. The stiffness values  $k_{\text{fou}}$ ,  $k_{\text{jack}}$  and  $k_{\text{pist}}$  determined from the in-situ tests, were taken for this model. The elements  $k_{j,j}$  of the matrix  $\mathbf{k}$  were compared with the values  $k_{j,j}$  determined during the in-situ tests.

The analysed model (Figure 8a) was composed of the reinforced concrete foundation slab, the steel tank, the jacks and the jack support. A slab of variable thickness in accordance with the survey (Figures 1 and 2) having elasticity modulus  $E_c = 28.3$  GPa, shear modulus  $G_c = 11.79$  GPa, the Poisson's ratio  $\nu = 0.2$  and weight density  $\gamma_c = 25$  kN/m<sup>3</sup>, was used as the model of reinforced concrete foundation slab (Figure 8b). A shell of 3 mm in thickness, made of the material having elasticity modulus  $E_s = 200$  GPa, shear modulus  $G_s = 76$  GPa, the Poisson's ratio  $\nu = 0.3$  and weight density  $\gamma_s = 78.5$  kN/m<sup>3</sup>, was used as the model of steel tank. The hinged connection was used as the connection between the foundation slab and the tank.

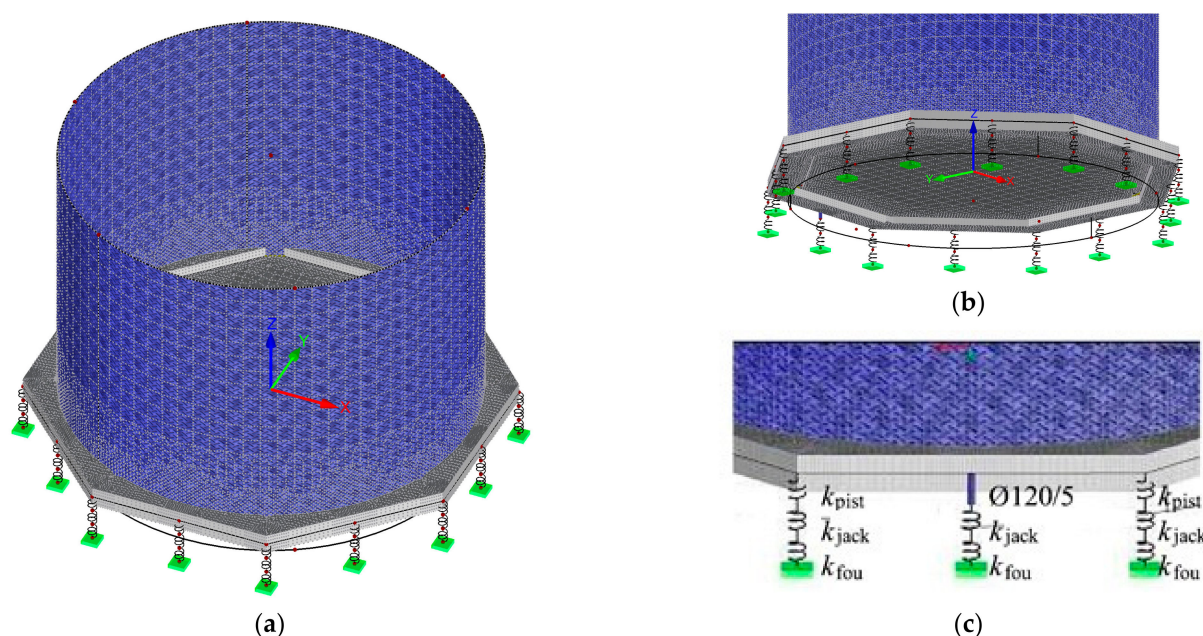


Figure 8. Tank model: (a) general view, (b) foundation slab; (c) passive supports and active support (inside).

The passive jacks were modelled with two stiffness values  $k_{\text{pist}}$  and  $k_{\text{jack}}$ , which were connected in series and modelled stiffness of the piston and the jack cylinder (Figure 8c). These stiffness values were taken on the basis of the in-situ tests. The model of the active jack was also composed of two elements: one element with stiffness  $k_{\text{jack}}$  which modelled piston cylinder and steel pipe having a diameter of 120 mm, wall thickness of 5 mm and length of 300 mm, which was used as the piston model. The support with stiffness  $k_{\text{fou}}$  was used as the model of the jack support.

## 4. Results from In-Situ Tests

The in-situ tests were conducted after preparing supports for the jacks; that is, after pressing stacks of concrete blocks into ground at each of  $n = 16$  points and removing water from the tank. The tank during the tests was placed on the supports which consisted of the jacks placed on their supports.

### 4.1. Stiffness of Support Elements

Changes in the force  $Q$  in the passive jack (1- Figure 6a) were caused by the forced

extension of pistons at the adjacent supports (3 and 15). Figure 9a presents three cycles of changes of the force  $Q$  within a range from  $Q_{\min}$  to  $Q_{\max}$ . Changes in the force  $Q$  in the passive jack resulted in: changes in free extension of the piston  $u_{\text{pist}}$  (Figure 9b), changes in the length of the jack cylinder  $\Delta l_{\text{jack}}$  (Figure 9c), and displacements of the jack support  $u_{\text{fou}}$  (Figure 9d). The maximum and minimum values  $u_{\text{pist}}$ ,  $\Delta l_{\text{jack}}$  and  $u_{\text{fou}}$  corresponding to the values  $Q_{\max}$  and  $Q_{\min}$  were determined for the loops shown in Figure 9b–d and compared in Table A1 (Appendix A). These values were used to determine stiffness  $k_{\text{pist}}$ ,  $k_{\text{jack}}$  and  $k_{\text{fou}}$  for each loop as changes in the force values ( $Q_{\max} - Q_{\min}$ ) divided by the relevant change ( $u_{\text{pist,max}} - u_{\text{pist,min}}$ ), ( $\Delta l_{\text{jack,max}} - \Delta l_{\text{jack,min}}$ ) and ( $u_{\text{fou,max}} - u_{\text{fou,min}}$ ). Moreover, Table A1 presents the adequate mean stiffness values for three loops which were as follows:  $k_{\text{pist}} = 110 \text{ MN/m}$ ,  $k_{\text{jack}} = 2579 \text{ MN/m}$  and  $k_{\text{fou}} = 150 \text{ MN/m}$ .

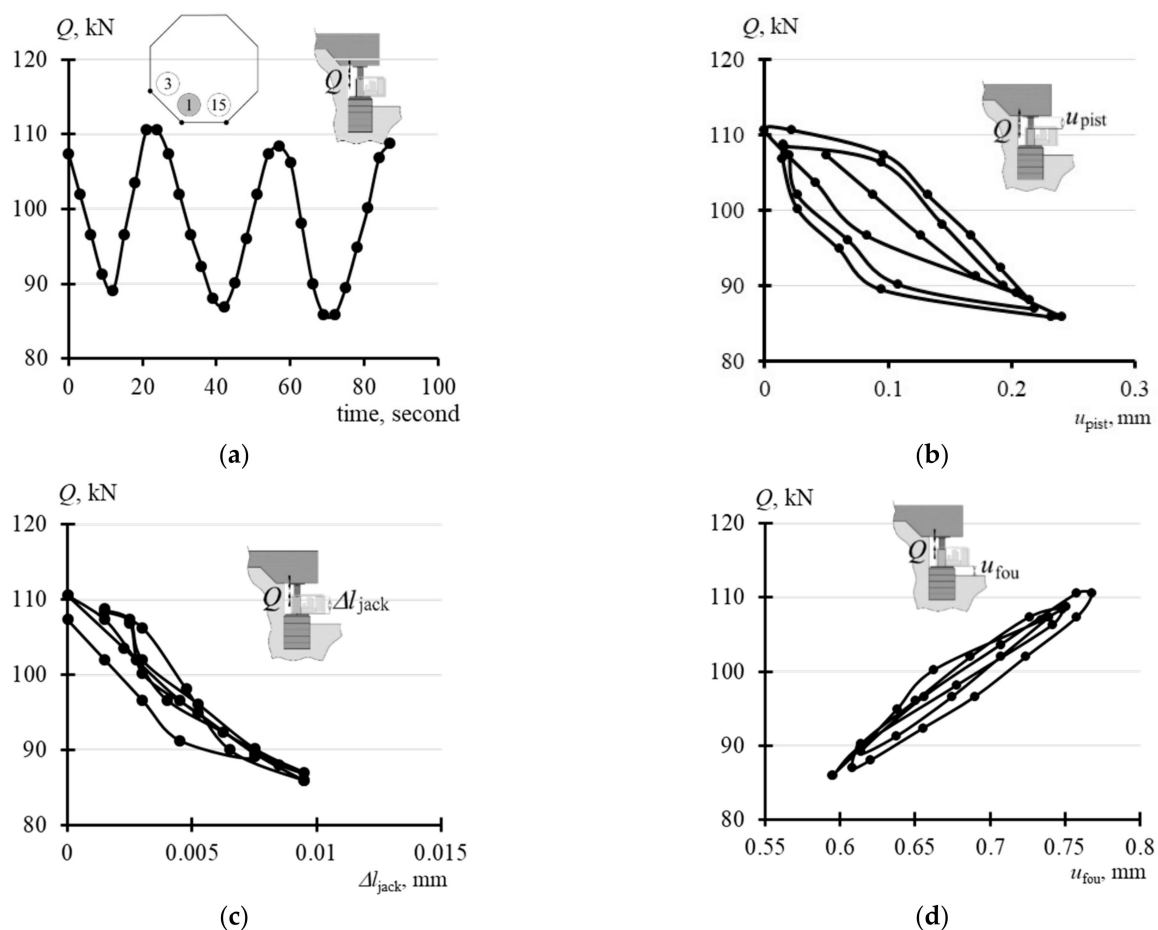


**Figure 9.** In-situ measurement results at the position of the passive jack: (a)  $Q$ —time; (b)  $Q$ — $u_{\text{pist}}$ ; (c)  $Q$ — $\Delta l_{\text{jack}}$ ; (d)  $Q$ — $u_{\text{fou}}$ ; 1, 3, 15—jack number.

#### 4.2. Stiffness of Rectified Tank

The extension  $u_{\text{ext},i}$  of the pistons was forced by a change in oil pressure in the consecutive jacks. Hence, for each  $n = 16$  jack placed under the tank, the forced extension of piston was equal to  $u_{\text{ext},j}$  ( $j = 1, \dots, 16$ ) as presented in Figure 10a. The corresponding changes in the force  $Q_{j,j}$  ( $j = 1, \dots, 16$ ) of the jacks are shown in Figure 10b. The values of piston extension before increasing oil pressure in the  $j$ -th jack were denoted as  $u_{\text{ext},j,\text{I}}$  and the extension after increasing oil pressure was denoted as  $u_{\text{ext},j,\text{II}}$ . The corresponding force values of the  $j$ -th jack were denoted as  $Q_{j,\text{I}}$  and  $Q_{j,\text{II}}$ .

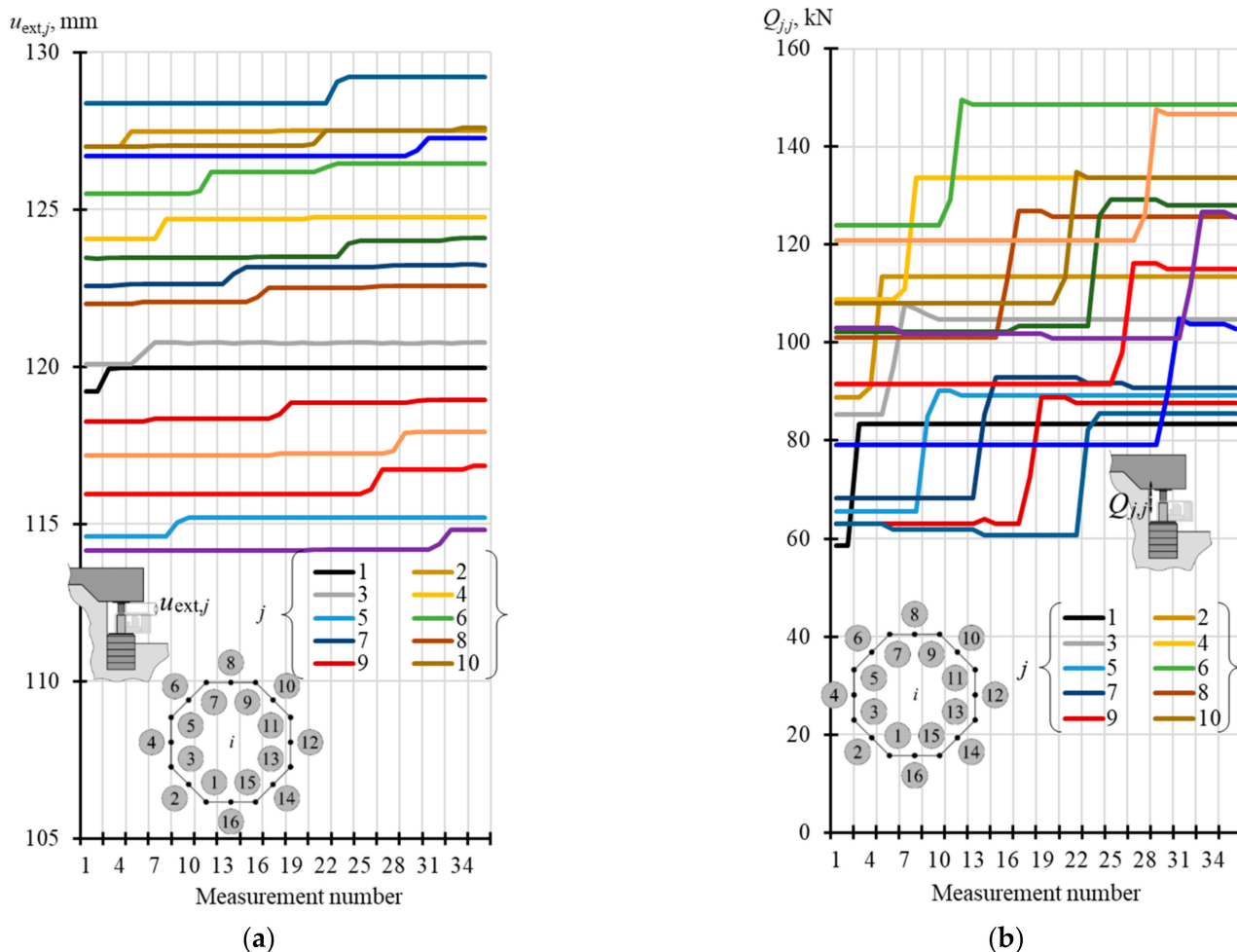


**Figure 10.** Results from in-situ tests for active supports (a) recorded forced piston extensions  $u_{ext,j}$ ; (b) recorded changes in forces  $Q_{j,j}$  in the jacks.

The values of  $Q_{j,I}$ ,  $Q_{j,II}$ ,  $u_{ext,j,I}$  and  $u_{ext,j,II}$  are compared in two tables. Table A2 (Appendix A) presents the values corresponding to the jacks installed in the corners of the foundation slab ( $j = 1, 3, 5, 7, 9, 11, 13, 15$ ), while the values corresponding to the jacks installed at the midpoint of the foundation side ( $j = 2, 4, 6, 8, 10, 12, 14, 16$ ) are summarised in Table A3 (Appendix A). Stiffness values  $k_{j,j}$  in these tables were determined as relevant values ( $Q_{j,j} = Q_{j,II} - Q_{j,I}$ ) divided by ( $u_{ext,j} = u_{ext,j,II} - u_{ext,j,I}$ ). The determined values  $k_{j,j}$  are displayed in Figure 11a. Figure 11b shows in blue mean stiffness values  $k_{j,j}$  corresponding to the jacks installed in the corners ( $k_{j,j,mean} = 38.10$  MN/m), and in red mean stiffness values  $k_{j,j}$  corresponding to the jacks installed at the midpoint of the side ( $k_{j,j,mean} = 46.36$  MN/m).

#### 4.3. Analysis of the Model

The calculations were made for this model taking into account stiffness of the support elements determined from the in-situ tests which were as follows:  $k_{pist} = 110$  MN/m,  $k_{jack} = 2579$  MN/m and  $k_{fou} = 150$  MN/m. They were used to verify correctness of the used numerical model of the rectified tank.

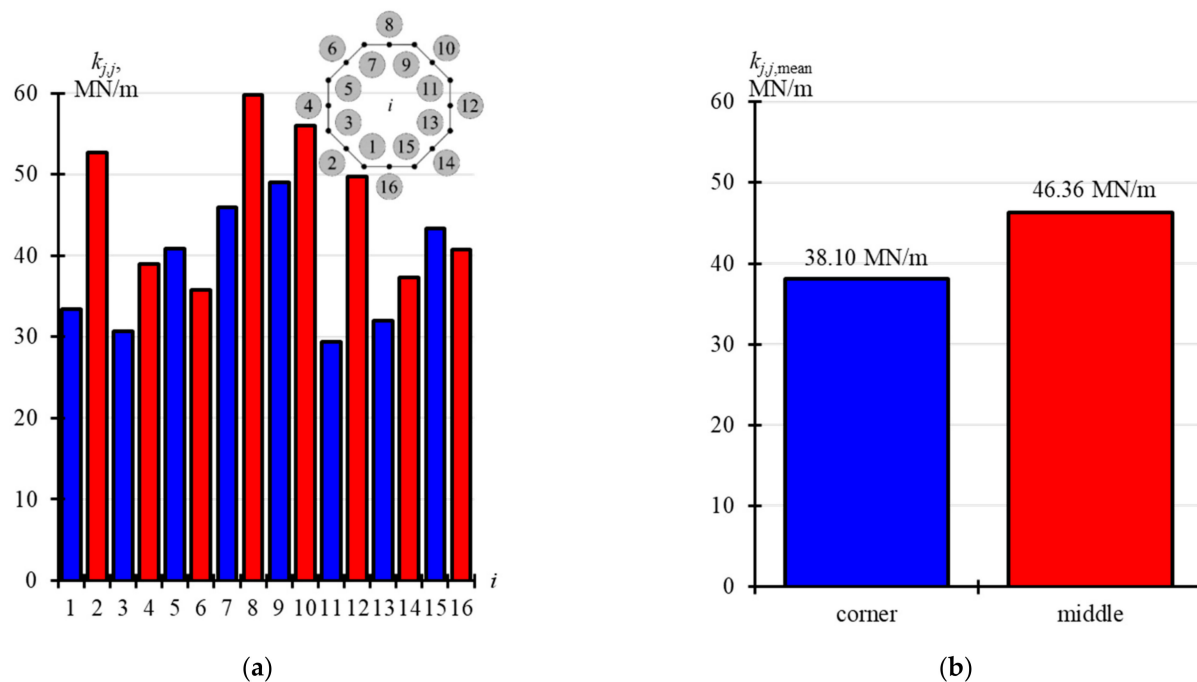


**Figure 11.** Results from in-situ tests for stiffness  $k_{jj}$ : (a) stiffness determined for  $n = 16$  supports; (b) mean stiffness values corresponding to points in the slab corners (corner) and at the mid-point of the slab side (middle).

The calculated results were the parameters  $\mathbf{k}$ ,  $\mathbf{f}_{obj}$  and  $\mathbf{f}_{fou}$  which formed the matrices, each in size of  $16 \times 16$ . Each  $j$ -th column was a vector corresponding to the effects produced by forced piston extension in the  $j$ -th jack by the unit value. The first column described the effects caused by the piston extension in the jack installed at the point  $j = 1$  by  $u_{ext,1} = 1$ , the second column specified the effects produced by the piston extension in the jack installed at the point  $j = 2$  by the unit value  $u_{ext,2} = 1$ , etc. Due to the structure symmetry, the column 3 related to the effects produced by the piston extension in the jack installed at the point  $j = 3$  had the same values as the first column. However, the values in the column 3 of the matrix were finally shifted by two positions with reference to the column 1 in such a way that for the matrix  $\mathbf{k}$  we obtain  $k_{1,1} = k_{3,3} = \dots = k_{15,15}$  and  $k_{2,2} = k_{4,4} = \dots = k_{16,16}$ . Thus, values of the elements from two columns defined each of the matrices  $\mathbf{k}$ ,  $\mathbf{f}_{obj}$  and  $\mathbf{f}_{fou}$ . For the matrix  $\mathbf{k}$  these values were  $k_{i,1}$  and  $k_{i,2}$  ( $i = 1, \dots, 16$ ), for the matrix  $\mathbf{f}_{obj}$  they were vectors  $\mathbf{f}_{obj,1}$  and  $\mathbf{f}_{obj,2}$  having values equal to  $f_{obj,i,1}$  and  $f_{obj,i,2}$  ( $i = 1, \dots, 16$ ), and for the matrix  $\mathbf{f}_{fou}$  they were vectors  $\mathbf{f}_{fou,1}$  and  $\mathbf{f}_{fou,2}$  of values  $f_{fou,i,1}$  and  $f_{fou,i,2}$  ( $i = 1, \dots, 16$ ). These values are summarised in Table A4 (Appendix A). While analysing the values of the stiffness matrix shown in this table, it should be emphasized that the experimentally determined value  $k_{j,j}$  for the model corresponding to the jack installed in the corner was equal to 37.260 MN/m, and the mean value  $k_{j,j}$  for  $j = 1, 3, \dots, 15$ , which was determined from the in-situ tests, was equal to 38.10 MN/m. Moreover, the calculated value  $k_{j,j}$  related to the jack installed at the mid-point of the foundation slab was 45.960 MN/m, and the relevant mean value  $k_{j,j}$  determined from the in-situ tests for  $j = 2, 4, \dots, 16$  was equal to 43.36 MN/m. Differences between these values which were experimentally obtained and determined for the model were equal to 6%, which was considered as the satisfactory conformity. These values presented in Table A4 are illustrated in Figures 12–14.

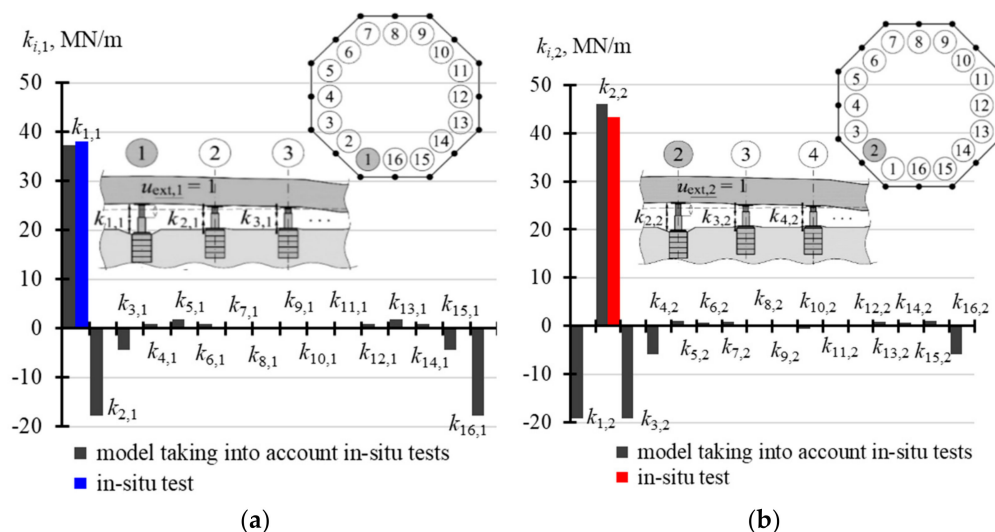


Figure 12. Values of elements in the matrix  $k$ : (a) elements  $k_{i,1}$ ; (b) elements  $k_{i,2}$ .

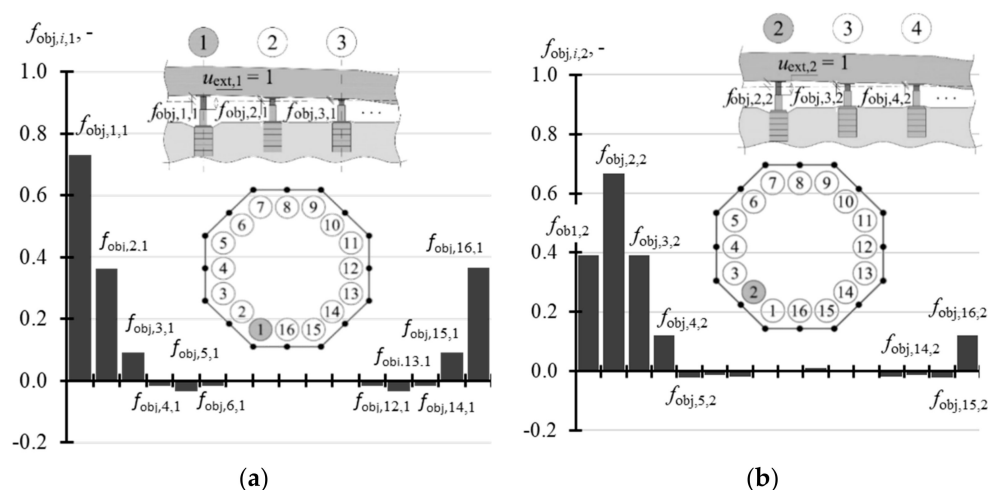


Figure 13. Values of elements in the matrix  $f_{obj}$ : (a) elements  $f_{obj,i,1}$ ; (b) elements  $f_{obj,i,2}$ .

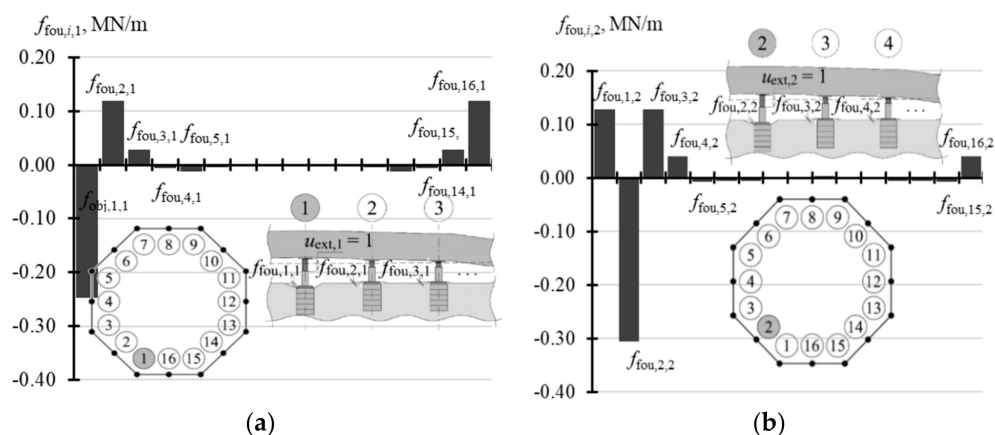


Figure 14. Values of elements in the matrix  $f_{fou}$ : (a) elements  $f_{fou,i,1}$ ; (b) elements  $f_{fou,i,2}$ .

The analysis of Figure 12 indicates that stiffness  $k_{2,2}$  was greater than stiffness  $k_{1,1}$ . Moreover, the forced displacement  $u_{ext,j}$  in the  $j$ -th active jack caused an increase in the force. Simultaneously, a drop in the force was observed for the adjacent passive jacks. While the force in the jack 1 was exerted, the force dropped in four adjacent jacks (elements  $k_{2,1}$ ,  $k_{3,1}$  and  $k_{16,1}$ ,  $k_{15,1}$  of negative values—Figure 12a). Accordingly, when force in the jack

2 was exerted, the force dropped also in four adjacent jacks (elements  $k_{1,2}$ ,  $k_{16,2}$  and  $k_{3,2}$ ,  $k_{4,2}$  of negative values—Figure 12b). A minor increase or drop in the force values was observed in other passive jacks.

Considering the value  $f_{\text{obj},i,j}$ , it could be concluded that at the point, at which the piston extension ( $i = j$ ) was forced, ca.70% of this extension ( $f_{\text{obj},1,1} = 0.730$ ,  $f_{\text{obj},2,2} = 0.667$ ) was transferred to the motion towards the top of the tank slab at that point. Moreover, the upward displacements were found for four adjacent points with reference to the points, at which the active jacks were operated (Figure 13a,b). Other points were shifted downwards or their displacement values were close to zero.

For the value  $f_{\text{fou},i,j}$ , the support for the jack, for which the extension  $u_{\text{ext},j} = 1$  of the piston ( $i = j$ ) was forced, was observed to be displaced downwards. This displacement was equal to  $f_{\text{fou},1,1} = 0.287$  for the jacks installed in the corners, and  $f_{\text{fou},1,1} = 0.306$  for the jacks installed at the mid-point of the side, which contributed to 28.7–30.6% of the forced value  $u_{\text{ext}}$ . The supports for four adjacent jacks were displaced upwards, while others did not move or were slightly displaced downwards (Figure 14a,b).

## 5. Analysis of the Structure Variables on Parameters of the Rectified Tank

The analysis further focused on the effect of variables  $n$  and  $k_{\text{fou}}$  of the model ( $n = 3, 4, 8, 16$  and  $32$ ,  $k_{\text{fou}} = 50$  MN/m, 100 MN/m, 150 MN/m, 200 MN/m, 250 MN/m and  $k_{\text{fou}}$ —rigid) on the matrices  $\mathbf{k}$ ,  $\mathbf{f}_{\text{obj}}$  and  $\mathbf{f}_{\text{fou}}$  of the structure, which was the tank on the jacks that were placed on the jack supports.

### 5.1. Stiffness Matrix

The stiffness matrix  $\mathbf{k}$  for the structure was a rectangular array of elements  $k_{i,j}$  of the size  $n \times n$ , where  $n$  is the number of the jacks, on which the tank was placed. For  $n = 3$ , all elements  $k_{i,j}$  were equal to zero, which means that the forced extension  $u_{\text{ext},j}$  in any  $j$ -th jack did not cause a change in the force  $Q_{i,j}$  in any support. In other cases ( $n > 3$ ), the diagonal elements  $k_{i,j}$  ( $i = j$ ) were always different than zero and took positive values, which means that the forced extension  $u_{\text{ext},j}$  of the jack piston at the  $j$ -th support caused an increase in the force  $Q_{j,j}$  ( $i = j$ ) in the  $j$ -th support. Other matrix elements could take negative, positive or zero values. For the element  $k_{i,j}$  lower than zero, the extension  $u_{\text{ext},j}$  caused a drop in the force in the  $i$ -th support.

When  $n = 4$ , the values of three elements of the matrix found in the first column:  $k_{1,1}$ ,  $k_{2,1}$  and  $k_{3,1}$  were sufficient for the explicit description of the matrix  $\mathbf{k}$ . The elements for the analysed stiffness  $k_{\text{fou}}$  of the supports are presented in Table A5 (Appendix A). Other elements from the first column, due to the symmetric arrangement of all jacks in the corners, could be determined by taking into account the matrix symmetry. Thus, the element  $k_{4,1}$  was equal to  $k_{2,1}$ . Additionally, all diagonal elements were equal to each other. Thus, other columns could be also determined as the matrix was symmetric.

A similar situation occurred when  $n = 8$ . Considering the position of the jacks in the slab corners, which was a regular hexagon, first five elements of the first column:  $k_{1,1}$ ,  $k_{2,1}$ ,  $k_{3,1}$ ,  $k_{4,1}$ ,  $k_{5,1}$  were sufficient to define the whole matrix. Other elements of the matrix were determined as all diagonal elements were equal and the matrix was symmetrical. The elements describing the matrix  $\mathbf{k}$ , when  $n = 8$ , for the analysed values  $k_{\text{fou}}$  are compared in Table A5 (Appendix A).

For  $n = 16$ , the matrix  $\mathbf{k}$  had two different vectors. The first element  $k_{i,1}$  ( $i = 1, \dots, 16$ ) defines changes in the values of forces in the supports caused by the unitary forced piston extension in the slab corner, and the second element  $k_{i,2}$  defines the values of forces in the supports caused by the unitary forced piston extension at the midpoint of the slab side. Each of the 16-element columns was clearly described by nine elements. Other elements of the first and second columns, and other columns could be determined from properties of the symmetric matrix taking into account that  $k_{1,1} = k_{3,3} = \dots = k_{15,15}$  and  $k_{2,2} = k_{4,4} = \dots = k_{16,16}$ . The elements describing the matrix  $\mathbf{k}$ , when  $n = 16$ , for the analysed values  $k_{\text{fou}}$  are compared in Table A6 (Appendix A).

Three columns had to be determined to define the matrix  $\mathbf{k}$  when  $n = 32$ . Each of these columns was clearly described by 17 elements. Data presented in Table A7 (Appendix A) were reduced to first nine values of the vectors  $k_{i,1}$ ,  $k_{i,2}$ ,  $k_{i,3}$ . The absolute value of other elements was lower than 3.27 MN/m.

The selected elements of the matrix  $\mathbf{k}$  for the analysed support stiffness  $k_{fou}$  are graphically presented in the following figures. Figure 15a illustrates the selected elements for  $n = 4$ , while Figure 15b shows the selected elements for  $n = 8$ . Figure 16a,b show selected elements  $k_{i,1}$  and  $k_{i,2}$  when  $n = 16$ . Figure 17a–c show selected elements of the columns  $k_{i,1}$ ,  $k_{i,2}$  and  $k_{i,3}$  for  $n = 32$ .

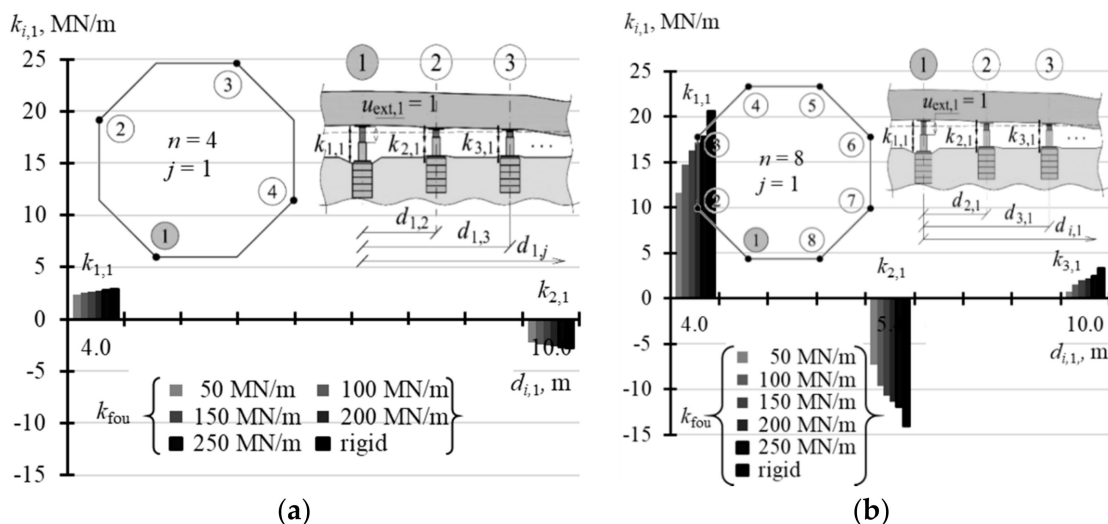


Figure 15. Selected elements of the stiffness matrix  $\mathbf{k}$  for the structure for different stiffness values  $k_{fou}$  of the jack supports for: (a)  $n = 4$ ; (b)  $n = 8$ .

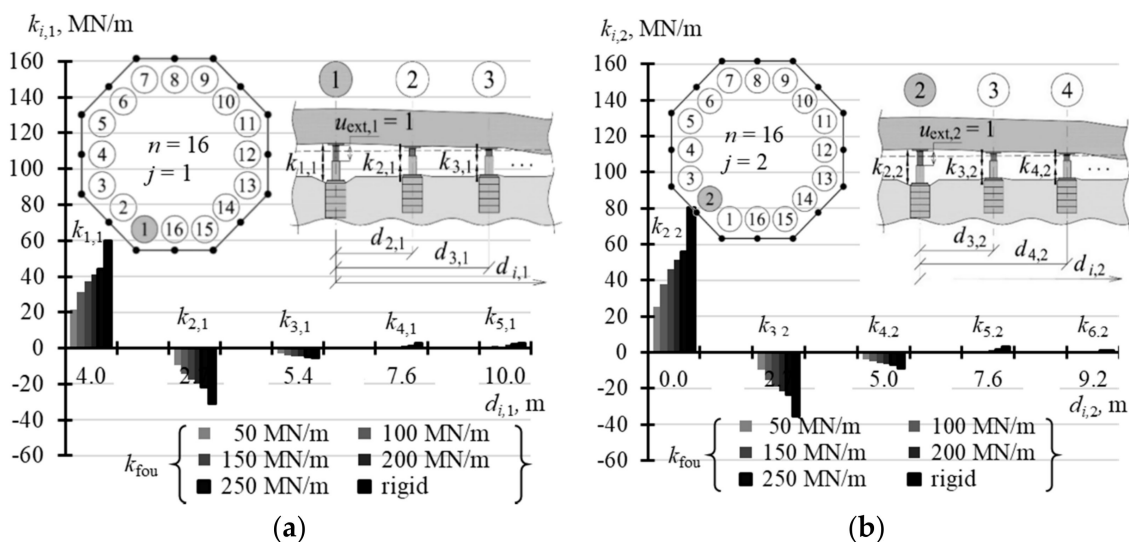
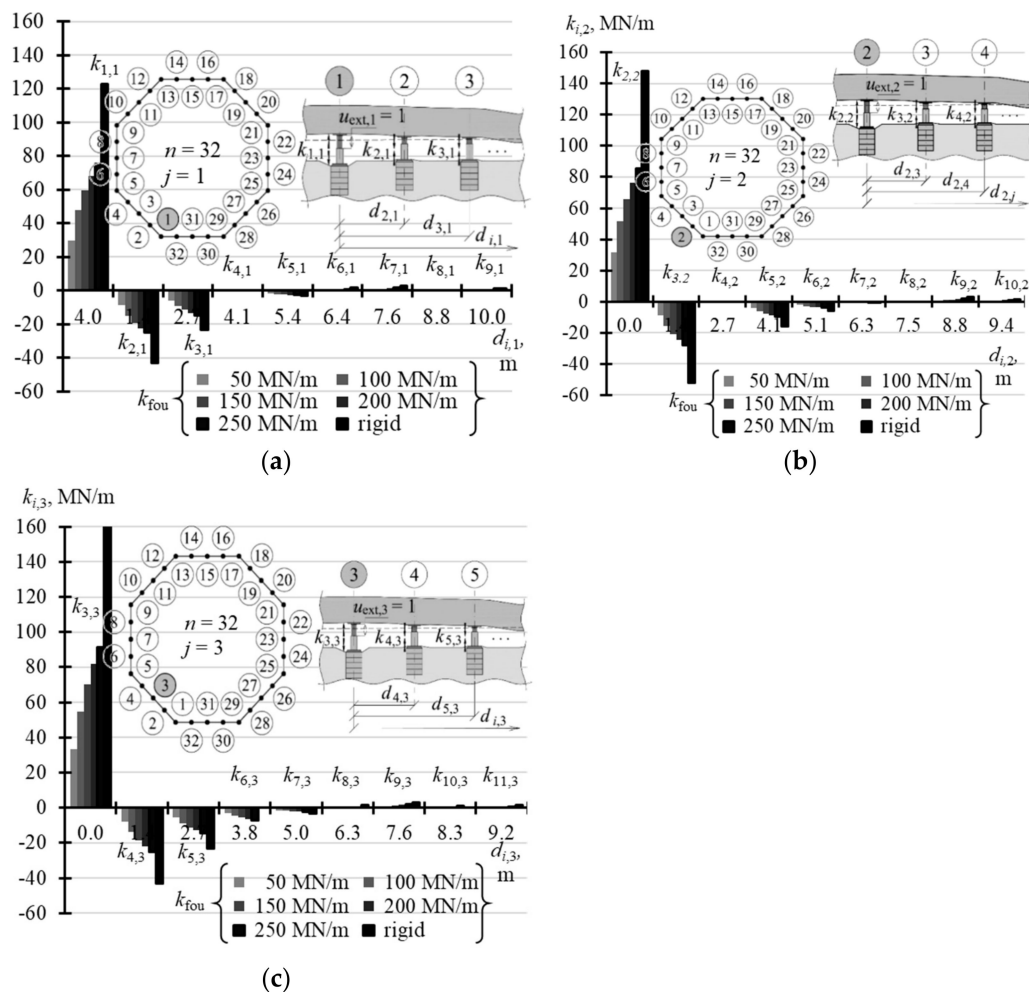


Figure 16. Selected elements of the stiffness matrix  $\mathbf{k}$  for the structure for different stiffness values  $k_{fou}$  of the jack supports when  $n = 16$ : (a) elements  $k_{i,1}$ ; (b) elements  $k_{i,2}$ .



**Figure 17.** Selected elements of the stiffness matrix  $\mathbf{k}$  for the structure for different stiffness values  $k_{fou}$  of the jack supports when:  $n = 32$ : (a) elements  $k_{i,1}$ ; (b) elements  $k_{i,2}$ ; (c) elements  $k_{i,3}$ .

With an increasing  $n$  number of the jacks, on which the tank was placed, the values of diagonal elements  $k_{j,j}$  were also increasing. At the same time, the structures of greater stiffness  $k_{fou}$  had higher values  $k_{j,j}$ . For  $n = 4$ , the values  $k_{1,1}$  corresponding to stiffness  $k_{fou} = 50$  MN/m were equal to 2.352 MN/m, and for the rigid support  $k_{1,1}$  were equal to 2.848 MN/m (Table A5 in Appendix A). Depending on the stiffness  $k_{fou}$ , for  $n = 8$ , the values  $k_{1,1}$  ranged from 11.6 MN/m to 20.583 MN/m (Table A5); for  $n = 16$  the values  $k_{1,1}$  ranged from 21.63 MN/m to 59.94 MN/m (Table A6 in Appendix A); and for  $n = 32$  the values  $k_{1,1}$  ranged from 29.79 MN/m to 122.72 MN/m (Table A7 in Appendix A). The columns of the matrix corresponding to forced piston excitation on the jacks at the midpoint of the foundation side had higher values  $k_{j,j}$ , for  $n = 16$  and  $n = 32$ .

By analysing the  $j$ -th column of the matrix, it should be noted that the elements next to the diagonal element  $k_{j,j}$  ( $i = j$ ) always took negative values. For  $n = 4$  and  $n = 8$ , two elements  $k_{i,i-1}$  and  $k_{i,i+1}$  adjacent to  $k_{j,j}$  took negative values, for  $n = 16$  six elements adjacent to  $k_{j,j}$  took negative values, and for  $n = 32$  eight elements adjacent to  $k_{i,i}$  took negative values.

### 5.2. Matrix of Displacement Forms of Elevated Tank

A structure of the matrix  $\mathbf{f}_{obj}$  displacement forms of the elevated tank was similar to the structure of the stiffness matrix. This means that the matrix could be defined without the need to write the whole elements. Therefore, Table A8 (Appendix A) shows the selected values  $f_{obj,i,1}$  of the vector  $\mathbf{f}_{obj,1}$  when  $n = 3, 4$ , and  $8$ , Table A9 (Appendix A) contains the selected values of vectors  $\mathbf{f}_{obj,1}$  and  $\mathbf{f}_{obj,2}$  for  $n = 16$ , and Table A10 (Appendix A) presents

the selected values of vectors  $f_{obj,1}$ ,  $f_{obj,2}$  and  $f_{obj,3}$  for  $n = 32$ . When  $n = 3$ , the elements  $f_{obj,j,j}$  ( $i = j$ ) took the value 1, and the other elements  $f_{obj,i,j}$  ( $i \neq j$ ) took the value 0 regardless of the support stiffness  $k_{fou}$ . In other cases, the values  $f_{obj,i,j}$  depended on stiffness  $k_{fou}$ . The values  $f_{obj,j,j}$  ( $i = j$ ) were higher for higher values  $k_{fou}$  and took lower values for a greater number  $n$  of the jacks. When  $n = 4$ ,  $f_{obj,j,j}$  ( $i = j$ ) took values from 0.952 to 0.998 (Figure 18a), and when  $n = 8$  from 0.731 to 0.988 (Figure 18b). When  $n = 16$ , the values  $f_{obj,j,j}$  corresponding to the jacks installed in the corner took values from 0.555 to 0.966 (Figure 19a), and values from 0.484 to 0.954 in case of the jacks at the midpoint of the side (Figure 19b). When  $n = 32$ , the values  $f_{obj,j,j}$  ( $i = j$ ) were within the range from 0.387 to 0.930 for the jacks in the corners (Figure 20a), from 0.350 to 0.916 for the jacks in  $1/4$  of the side length (Figure 20b), and from 0.318 to 0.907 for the jacks in  $1/2$  of the side length (Figure 20c).

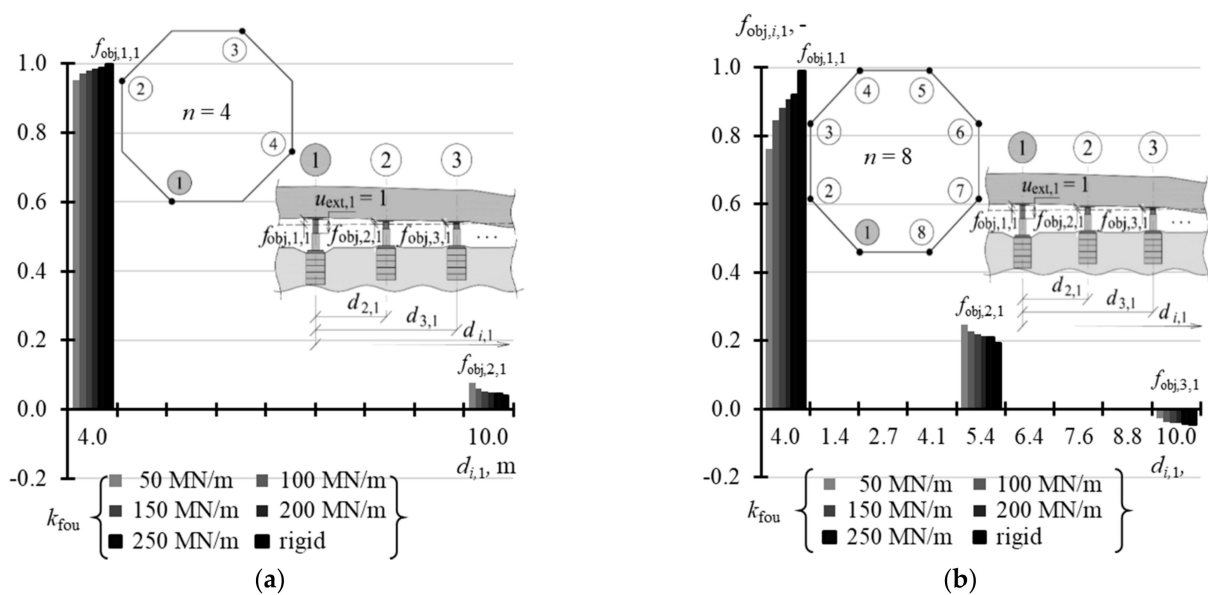


Figure 18. Elements of the matrix  $f_{obj}$  for different stiffness values  $k_{fou}$  of the jack support for: (a)  $n = 4$ ; (b)  $n = 8$ .

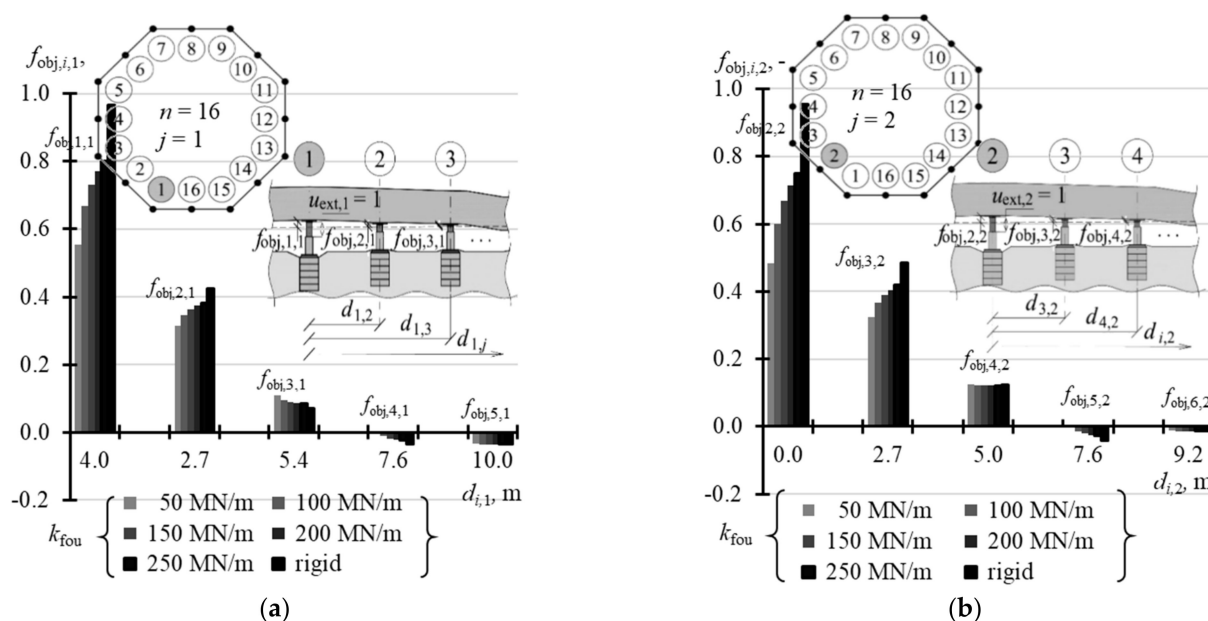
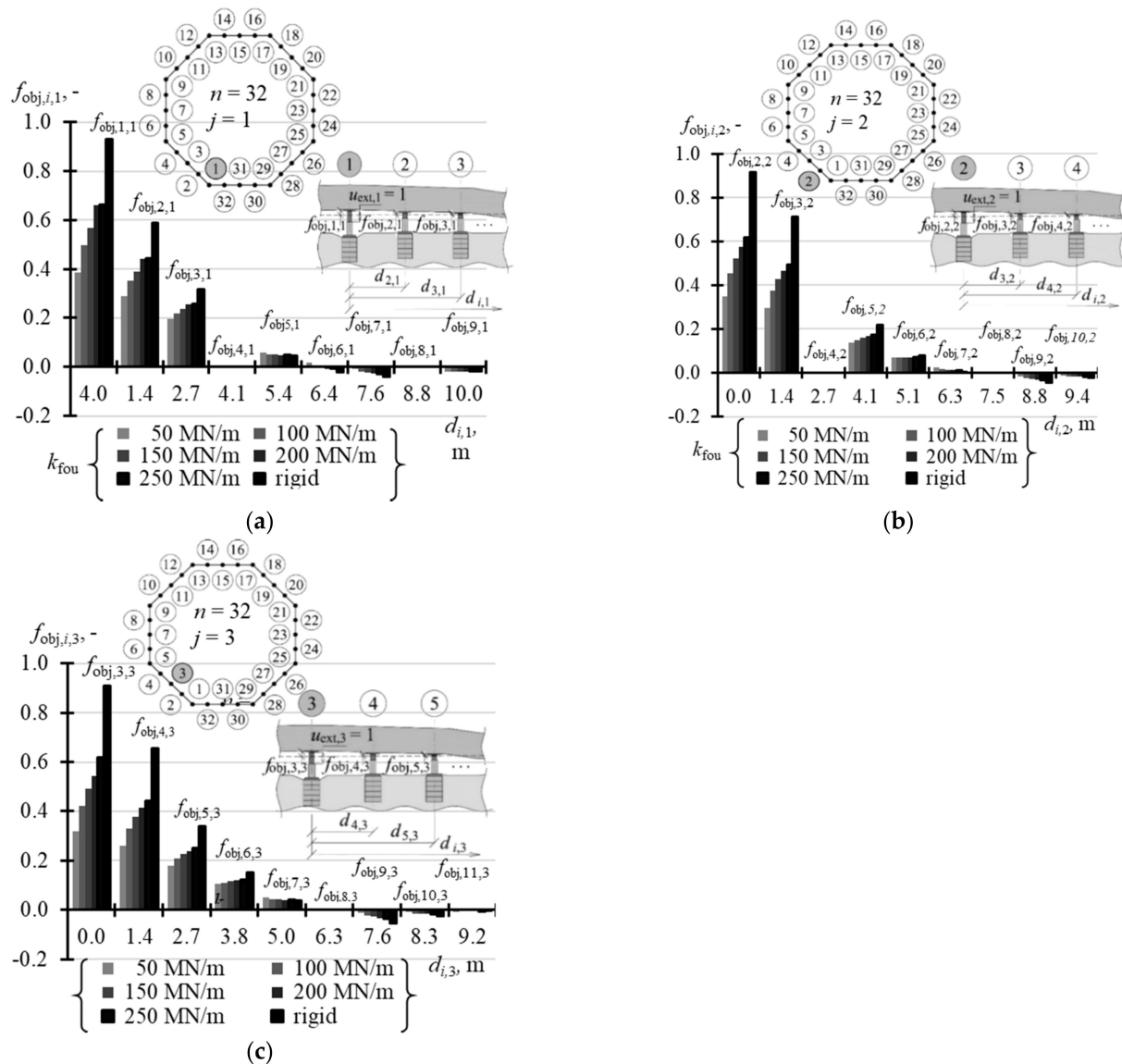


Figure 19. Elements of the matrix  $f_{obj}$  for different stiffness values  $k_{fou}$  of the jack support when  $n = 16$ : (a) elements  $f_{obj,i,1}$ ; (b) elements  $f_{obj,i,2}$ .



**Figure 20.** Elements of the matrix  $f_{obj}$  for different stiffness values  $k_{fou}$  of the jack support when  $n = 32$ : (a) elements  $f_{obj,i,1}$ ; (b) elements  $f_{obj,i,2}$ ; (c) elements  $f_{obj,i,3}$ .

### 5.3. Matrix of Displacement Forms of Jack Supports

The last test parameter of the tank was the matrix  $f_{fou}$  of displacement forms of jack supports, whose elements specified vertical displacements of the jack supports.

For  $n = 3$ , the elements  $f_{obj,i,j}$  took the value 0 regardless of the support stiffness  $k_{fou}$  (Table A11 in Appendix A). In other cases, the values  $f_{fou,i,j}$  depended on stiffness  $k_{fou}$ . The values  $f_{fou,j,j}$  ( $i = j$ ) were higher for lower values  $k_{fou}$  and took higher values for a greater number  $n$  of the jacks. When  $n = 4$ ,  $f_{fou,j,j}$  ( $i = i$ ) took values from  $-0.047$  to  $-0.011$  (Figure 21a), and when  $n = 8$  from  $-0.232$  to  $-0.070$  (Figure 21b). The elements of vectors  $f_{fou,1}$  and  $f_{fou,2}$  for  $n = 16$  are compared in Table A12 (Appendix A). The values  $f_{fou,j,j}$  ( $i = j$ ) corresponding to the jacks installed in the corner took values from  $-0.433$  to  $-0.173$  (Figure 22a), and from  $-0.484$  to  $-0.219$  for the jacks at the midpoint of the side (Figure 22b). When  $n = 32$  (Table A13 in Appendix A), the values  $f_{obj,j,j}$  ( $i = j$ ) were within the range from  $-0.596$  to  $-0.296$  for the jacks in the corners (Figure 23a), from  $-0.632$  to  $-0.334$  for the jacks in  $1/4$  of the side length (Figure 23b), and from  $-0.663$  to  $0.359$  for the jacks in  $1/2$  of the side length (Figure 23c). The values  $f_{fou,i,j}$  ( $i \neq j$ ) were higher or lower than zero. Higher absolute values  $f_{obj,i,j}$  ( $i \neq j$ ) were determined for lower values  $k_{fou}$ , regardless of the number of jacks.

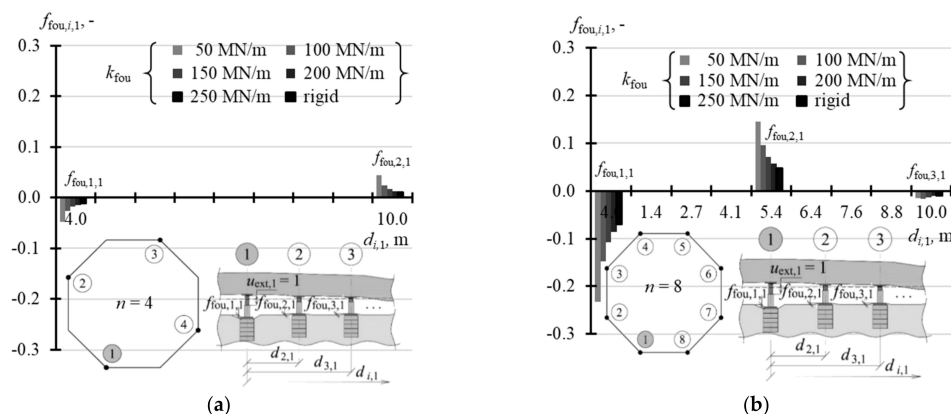


Figure 21. Elements of the matrix  $f_{fou}$  of support displacements for different stiffness values  $k_{fou}$  of the jack support: (a)  $n = 4$ ; (b)  $n = 8$ .

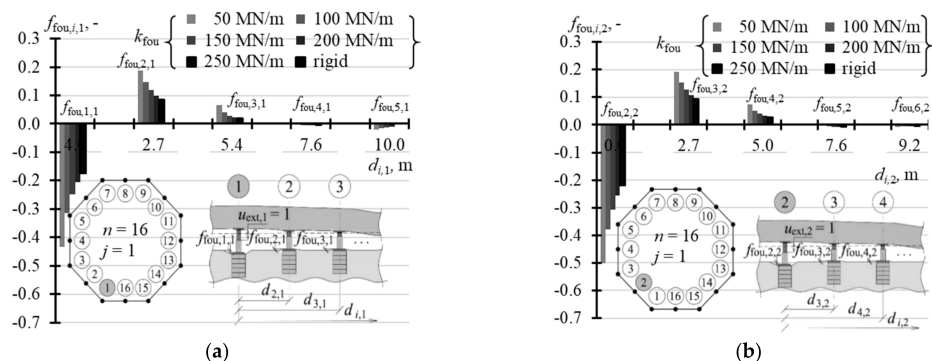


Figure 22. Elements of the matrix  $f_{fou}$  of support displacements for different stiffness values  $k_{fou}$  of the jack support when  $n = 16$ : (a) elements  $f_{fou,i,1}$ ; (b) elements  $f_{fou,i,2}$ .

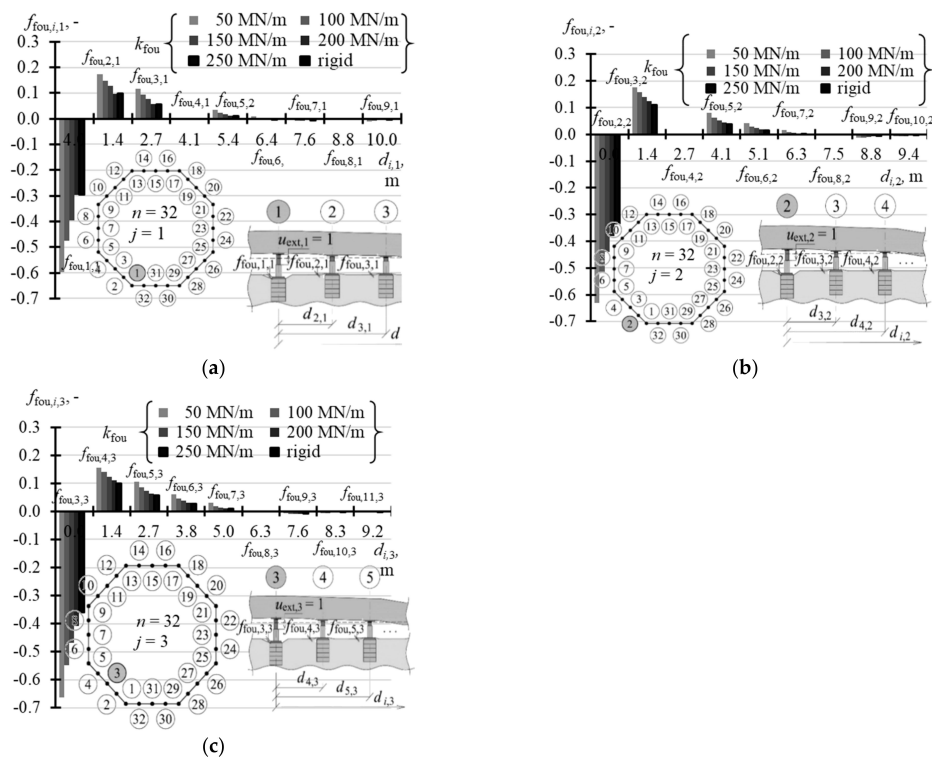


Figure 23. Elements of the matrix  $f_{fou}$  of support displacements for different stiffness values  $k_{fou}$  of the jack support when  $n = 32$ : (a) elements  $f_{fou,i,1}$ ; (b) elements  $f_{fou,i,2}$ ; (c) elements  $f_{fou,i,3}$ .

### 6. Analysis of Work Performed by Jacks

The further analysis focused on the forced piston extension  $u_{ext,j}$  by 1 mm, which was the same for all the jacks. For  $n = 3$ , the mean displacement of the structure  $u_{obj-mean}$  determined from the relationship

$$u_{obj-mean} = \frac{1}{n} \sum_{i=1}^n \sum_{j=1}^n f_{obj,i,j} u_{ext,j} \tag{20}$$

was equal to 1 mm. In other cases,  $u_{obj-mean}$  determined from the relations (20) depended on both the  $n$  number of the jacks and the support stiffness  $k_{fou}$ , and  $u_{obj-mean}$  was increasing as stiffness  $k_{fou}$  and the jack number  $n$  were increasing (Table A14 in Appendix A). When  $n = 4$ , then  $u_{obj-mean}$  ranged from 1.031 mm to 1.038 mm; when  $n = 8$ ,  $u_{obj-mean}$  took values from 1.151 mm to 1.272 mm; when  $n = 16$ ,  $u_{obj-mean}$  ranged from 1.307 mm to 1.923 mm; and when  $n = 32$ ,  $u_{obj-mean}$  took values from 1.414 mm to 2.911 mm (Figure 24a). Assuming that the force  $Q_{g,i}$ , the values of which for the analysed variables are shown in Table A15 (Appendix A), was acting on each active support prior to the forced extension  $u_{ext}$  of the pistons, then the work  $W_{jack,j}$  performed by the  $j$ -th active jack during the piston extension by  $u_{ext} = 1$  mm depended on the number  $n$  of supports. Moreover, for  $n = 16$  and 32, work  $W_{jack,j}$  depended also on the support stiffness  $k_{fou}$  (Figure 24b). Higher values  $W_{jack,j}$  were obtained for higher values  $k_{fou}$ . For the jacks installed in the corner, the work took the following values: 0.458 kJ at  $n = 3$ , 0.338 kJ at  $n = 4$ , from 0.176 kJ to 0.179 kJ at  $n = 8$ , from 0.075 kJ to 0.076 kJ at  $n = 16$ , and from 0.037 kJ to 0.057 kJ at  $n = 32$ .

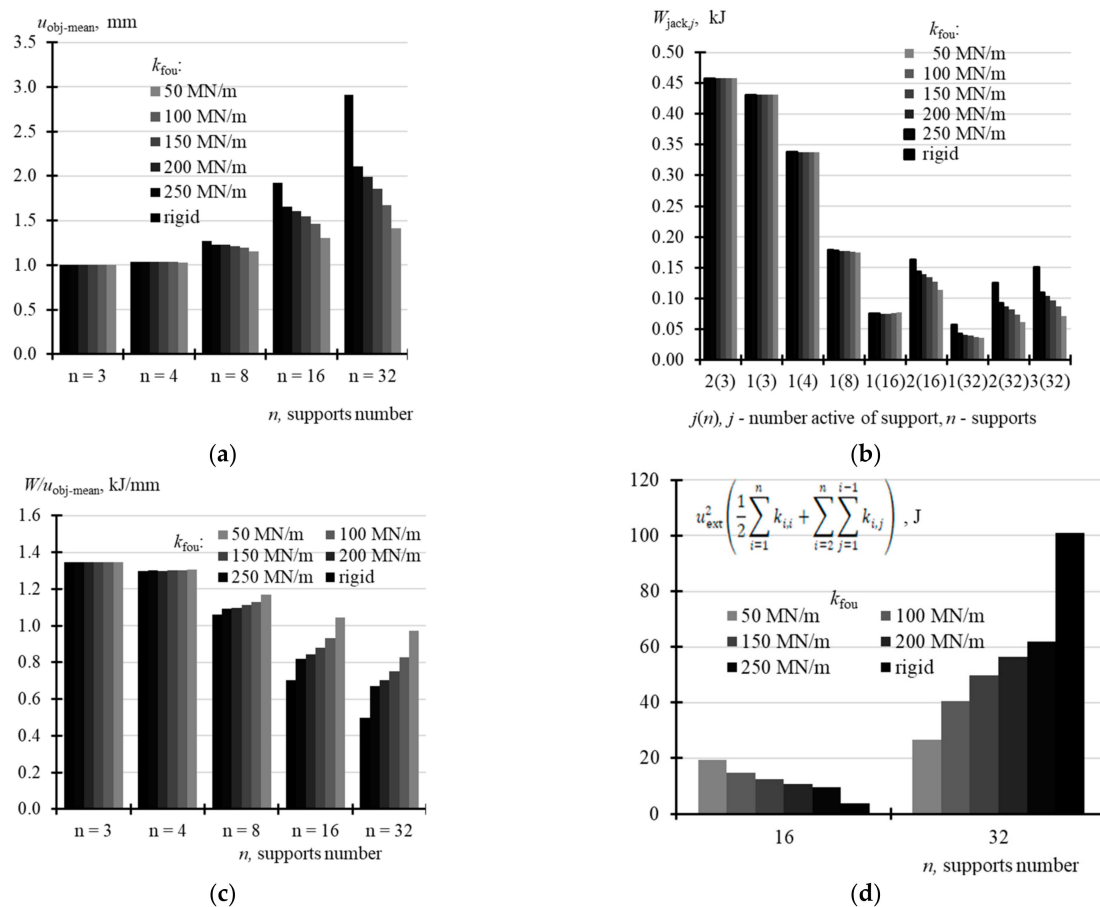


**Figure 24.** Analysed displacements of the tank and the work performed by the jacks: (a) mean displacements  $u_{obj-mean}$  derived from the Equation (20) at  $u_{ext,j} = 1$  mm ( $j = 1, \dots, n$ ); (b) work  $W_{jack,j}$  performed by the active jack; (c) work  $W$  obtained from (19) divided by mean displacements  $u_{obj-mean}$  from (20); (d) elastic energy of the deformed slab after forced displacements  $u_{ext,j} = 1$  mm ( $j = 1, \dots, n$ ) of pistons in all the jacks.

The total work  $W$  done by all the jacks during the piston extensions  $u_{ext} = 1$  mm and determined from the relationship (19) was the same for  $n = 3, 4$  and  $8$  jacks, did not depend on  $k_{fou}$  and was equal to  $1.347$  kJ. For  $n = 16$ , this work depended on stiffness  $k_{fou}$  and was equal to  $1.366$  kJ at  $k_{fou} = 50$  MN/m and  $1.350$  kJ at the rigid support (Table A14). For  $n = 32$ , this work was equal to  $1.373$  Mn/m at  $k_{fou} = 50$  MN/m, and equal to  $1.448$  MN/m at the rigid support. These differences were a consequence of elastic deformation, to which the structure was subjected after the forced extension  $u_{ext}$  of all pistons. Displacements  $u_{obj,i}$  of the points on the slabs and displacements  $u_{fou,i}$  of the jack supports after forced extension of the pistons  $u_{ext,j} = 1$  ( $j = 1, \dots, n$ ) are illustrated in Figure 25a for  $k_{fou} = 50$  MN/m, and in Figure 25b for the rigid support.

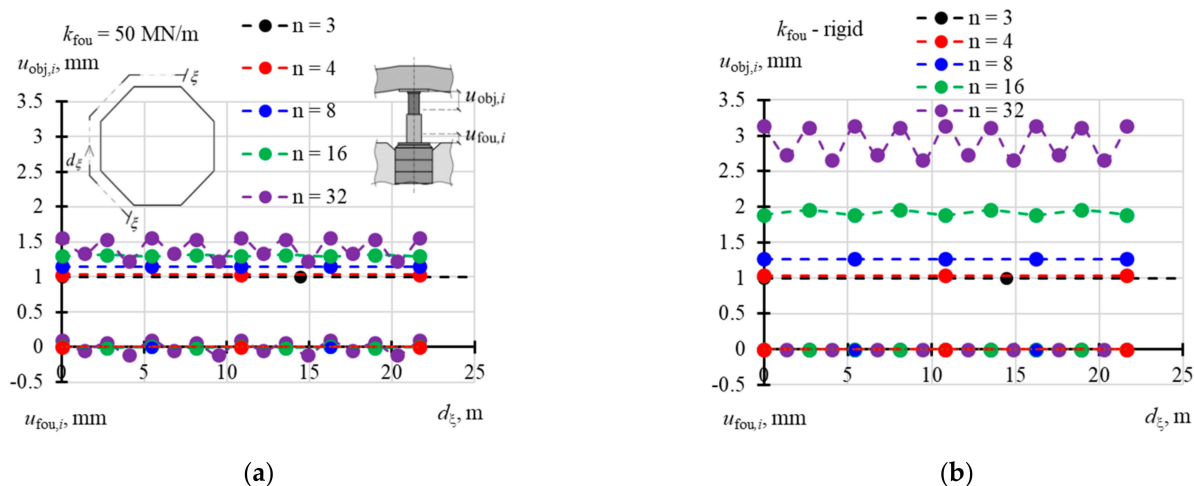


**Figure 25.** Displacements of the object at points  $i$  ( $u_{obj,i}$ ) and displacements of the support of the  $i$ -th jack ( $u_{fou,i}$ ) after forced extensions of all the jack pistons  $u_{ext,j} = 1$  mm ( $j = 1, \dots, n$ ): (a)  $k_{fou} = 50$  MN/m; (b) rigid support for the jacks.

Table A14 shows the values of work described by the Equation (19) divided by the mean displacement  $u_{obj-mean}$  expressed as (20). This comparison indicates that lifting the building by 1 mm required the least energy when the number of supports was  $n = 32$  and the jack support was rigid. Then, the result was  $0.497$  kJ/mm. Lifting the structure by 1 mm required the highest energy for  $n = 3$  jacks. Then, the result was  $1.367$  kJ/mm. It can be concluded that installing a significant number of the jacks and providing the rigid jack support for them was the most favourable conditions during the rectification.

### 7. Conclusions

The parameters of the rectified tank placed on  $n$  hydraulic piston jacks installed under the tank were described using three matrices: stiffness matrix  $\mathbf{k}$ , matrix  $\mathbf{f}_{obj}$  of displacement forms of elevated tank, and matrix  $\mathbf{f}_{fou}$  of displacement forms of jack supports.

When  $n = 3$ , the structure was statically determinate. Hence, the matrices  $\mathbf{k}$  and  $\mathbf{f}_{fou}$  had entries equal to zero, and the matrix  $\mathbf{f}_{obj}$  was the identity matrix. With an increasing number  $n$  of the jacks, on which the tank was placed, the values of diagonal elements  $k_{j,j}$  were also increasing. At the same time, the structures of greater stiffness  $k_{fou}$  had higher values  $k_{j,j}$ . For  $n = 4$ , the values  $k_{j,j}$  corresponding to stiffness  $k_{fou} = 50$  MN/m were equal to  $2.352$  MN/m, and  $2.848$  MN/m for the rigid support  $k_{fou}$ . For  $n = 32$ , the values  $k_{j,j}$  ranged from  $29.79$  MN/m to  $122.72$  MN/m. The values  $k_{i,j}$  ( $i \neq j$ ) were lower for a greater number of the jacks and higher stiffness values  $k_{fou}$ , which meant a bigger drop in forces in the active support at the same forced extension  $u_{ext}$ .

The values  $f_{obj,j,j}$  ( $i = j$ ) were higher for higher stiffness values  $k_{fou}$  and took lower values for a greater  $n$  number of the jacks. For  $n = 4$ ,  $f_{obj,j,j}$  ( $i = j$ ) took values from  $0.952$  to  $0.998$ . For  $n = 32$ , the values  $f_{obj,j,j}$  ( $i = j$ ) were within a range of  $0.335$ – $0.930$ .

The conducted energy analysis demonstrated that as the  $n$  number of jacks and stiffness  $k_{fou}$  were increasing, the amount of work required to provide the vertical displacement

of the object was decreasing. For  $n = 3$ , the work required to elevate the object by 1 mm was 1.347 kJ. For  $n = 32$  and the rigid support for the jacks, 0.497 kJ of energy was sufficient to elevate the object by 1 mm. Thus, it can be concluded that installing a significant number of the jacks and providing the rigid jack support for them was the most favourable condition during the rectification. On the other hand, increasing the number of jacks increases the investment cost. For this reason, the number of jacks used for the tank rectification was limited to 16.

**Funding:** This research was funded by Silesian University of Technology; Grant No. 03/020/RGJ21/0102.

**Institutional Review Board Statement:** Not applicable.

**Informed Consent Statement:** Not applicable.

**Data Availability Statement:** Not applicable.

**Acknowledgments:** I would like to thank the MPL company from Katowice, Poland for the technical support of the research carried out in-situ.

**Conflicts of Interest:** The author declares no conflict of interest.

## Appendix A

**Table A1.** Extreme values:  $Q$ ,  $u_{\text{pist}}$ ,  $\Delta l_{\text{jack}}$  and  $u_{\text{fou}}$  determined from subsequent load cycles of the passive support during the in-situ tests and stiffness of the support elements  $k_{\text{pist}}$ ,  $k_{\text{jack}}$ ,  $k_{\text{fou}}$  determined on their basis.

Loop	$Q_{\text{max}}$	$u_{\text{pist,min}}$	$\Delta l_{\text{jack,min}}$	$u_{\text{fou,min}}$	$k_{\text{pist}}$	$k_{\text{jack}}$	$k_{\text{fou}}$
	$Q_{\text{min}}$	$u_{\text{pist,max}}$	$\Delta l_{\text{jack,max}}$	$u_{\text{fou,max}}$			
	[kN]	[mm]	[mm]	[mm]			
1	107.36	0.049	0.000	0.740	118	2433	145
	89.11	0.204	0.008	0.614			
2	110.58	0.000	0.000	0.758	108	2486	158
	86.96	0.218	0.010	0.608			
3	108.43	0.016	0.002	0.748	104	2818	147
	85.89	0.232	0.010	0.595			
mean values					110	2579	150

**Table A2.** Stiffness  $k_{j,j}$  determined from in-situ tests according to (1) at points at the foundation corners.

$i = j$	1	3	5	7	9	11	13	15
$Q_{j,I}$ , kN	58.63	85.31	65.56	68.17	62.98	60.77	91.45	79.09
$Q_{j,II}$ , kN	83.32	105.71	90.25	92.86	88.75	85.47	116.14	103.78
$Q_{j,j} = Q_{j,II} - Q_{j,I}$ , kN	24.69	20.40	24.69	24.69	25.77	24.69	24.69	24.69
$u_{\text{ext},j,I}$ , mm	119.23	120.10	114.59	122.64	118.35	128.38	115.96	126.70
$u_{\text{ext},j,II}$ , mm	119.97	120.76	115.20	123.18	118.87	129.22	116.74	127.27
$u_{\text{ext},j} = u_{\text{ext},j,II} - u_{\text{ext},j,I}$ , mm	0.74	0.67	0.60	0.54	0.53	0.84	0.77	0.57
$k_{j,j}$ MN/m	33.44	30.66	40.87	45.98	49.05	29.43	31.99	43.28

**Table A3.** Stiffness  $k_{jj}$  determined from in-situ tests according to (1) at points at mid-points of the sides.

$i = j$	2	4	6	8	10	12	14	16
$Q_{j,I}$ , kN	88.84	108.84	123.84	101.05	107.95	103.32	120.77	100.80
$Q_{j,II}$ , kN	113.54	133.54	148.53	126.82	133.72	129.09	146.54	126.57
$Q_{jj} = Q_{j,II} - Q_{j,I}$ , kN	24.69	24.69	24.69	25.77	25.77	25.77	25.77	25.77
$u_{ext,j,I}$ , mm	127.00	124.06	125.49	122.07	127.04	123.50	117.24	114.19
$u_{ext,j,II}$ , mm	127.47	124.69	126.18	122.50	127.50	124.02	117.93	114.82
$u_{ext,j} = u_{ext,j,II} - u_{ext,j,I}$ , mm	0.47	0.63	0.69	0.43	0.46	0.52	0.69	0.63
$k_{jj}$ MN/m	52.68	38.94	35.82	59.71	55.98	49.76	37.32	40.71

**Table A4.** Tank parameters calculated for  $n = 16$  and  $k_{jack} = 2579$  MN/m,  $k_{pist} = 110$  MN/m and  $k_{fou} = 150$  MN/m (elements, for which  $i = j$ , that is,  $k_{ij}$ ,  $f_{obj,ij}$  and  $f_{fou,ij}$  are given in bold).

$i$	$k_{i,1}$ , MN/m	$k_{i,2}$ , MN/m	$f_{obj,i,1}$ -	$f_{obj,i,2}$ -	$f_{fou,i,1}$ -	$f_{fou,i,2}$ -
1	<b>37.260</b>	-19.142	<b>0.730</b>	0.390	<b>-0.248</b>	0.128
2	-17.853	<b>45.960</b>	0.363	<b>0.667</b>	0.119	<b>-0.306</b>
3	-4.407	-19.142	0.090	0.390	0.029	0.128
4	0.882	-5.943	-0.018	0.121	-0.006	0.040
5	1.765	1.019	-0.036	-0.021	-0.012	-0.007
6	0.794	0.702	-0.016	-0.014	-0.005	-0.005
7	0.238	0.896	-0.005	-0.018	-0.002	-0.006
8	-0.009	-0.281	0.000	0.006	0.000	0.002
9	-0.071	0.024	0.001	0.000	0.000	0.000
10	-0.009	-0.508	0.000	0.010	0.000	0.003
11	0.239	0.022	-0.005	0.000	-0.002	0.000
12	0.795	-0.28	-0.016	0.006	-0.005	0.002
13	1.764	0.896	-0.036	-0.018	-0.012	-0.006
14	0.884	0.702	-0.018	-0.014	-0.006	-0.005
15	-4.409	1.019	0.090	-0.021	0.029	-0.007
16	-17.858	-5.944	0.364	0.121	0.119	0.040

**Table A5.** Values  $k_{ij}$  of stiffness matrix  $k$  expressed in MN/m, for  $n = 3$ ,  $n = 4$  and  $n = 8$  and  $k_{fou} = 50, 100, 150, 200, 250$  MN/m and  $k_{fou}$ -rigid (elements  $k_{ij}$  ( $i = j$ ) are given in bold).

$n$	$k_{ij}$	$k_{fou}$ , MN/m					Rigid
		50	100	150	200	250	
3	$k_{1,1}$	0	0	0	0	0	0
	$k_{1,2}$	0	0	0	0	0	0
4	$k_{1,1}$	<b>2.352</b>	<b>2.576</b>	<b>2.66</b>	<b>2.705</b>	<b>2.735</b>	<b>2.848</b>
	$k_{2,1}$	-2.258	-2.478	-2.561	-2.605	-2.634	-2.746
	$k_{3,1}$	2.164	2.381	2.463	2.506	2.534	2.644
8	$k_{1,1}$	<b>11.6</b>	<b>14.747</b>	<b>16.257</b>	<b>17.145</b>	<b>17.778</b>	<b>20.583</b>
	$k_{2,1}$	-7.303	-9.602	-10.726	-11.393	-11.87	-14.004
	$k_{3,1}$	0.773	1.558	1.979	2.237	2.426	3.306
	$k_{4,1}$	0.699	0.737	0.728	0.715	0.701	0.606
	$k_{5,1}$	0.061	-0.134	-0.218	-0.263	-0.293	-0.402

**Table A6.** Values  $k_{i,j}$  of stiffness matrix  $\mathbf{k}$  expressed in MN/m, for  $n = 16$  and  $k_{\text{fou}} = 50, 100, 150, 200, 250$  MN/m and  $k_{\text{fou}}$ -rigid (elements  $k_{j,j}$  ( $i = j$ ) are given in bold).

$i$	$k_{\text{fou}}, \text{MN/m}$											
	50		100		150		200		250		Rigid	
	$k_{i,1}$	$k_{i,2}$	$k_{i,1}$	$k_{i,2}$	$k_{i,1}$	$k_{i,2}$	$k_{i,1}$	$k_{i,2}$	$k_{i,1}$	$k_{i,2}$	$k_{i,1}$	$k_{i,2}$
1	<b>21.63</b>	-9.65	<b>31.48</b>	-15.45	<b>37.26</b>	-19.14	<b>41.08</b>	-21.69	<b>44.03</b>	-23.71	<b>59.94</b>	-35.47
2	-9.34	<b>25.07</b>	-14.62	<b>37.96</b>	-17.85	<b>45.96</b>	-20.02	<b>51.42</b>	-21.71	<b>55.72</b>	-30.99	<b>80.44</b>
3	-3.23	-9.65	-4.04	-15.45	-4.41	-19.14	-4.61	-21.69	-4.75	-23.71	-5.29	-35.47
4	-0.09	-3.71	0.49	-5.15	0.88	-5.94	1.16	-6.46	1.38	-6.85	2.63	-8.90
5	0.98	-0.06	1.50	0.57	1.77	1.02	1.93	1.34	2.04	1.60	2.57	3.17
6	0.58	0.36	0.73	0.59	0.79	0.70	0.83	0.76	0.86	0.80	0.98	0.93
7	0.30	0.62	0.27	0.81	0.24	0.90	0.22	0.95	0.20	0.99	0.09	1.21
8	0.01	0.01	-0.01	-0.16	-0.01	-0.28	0.00	-0.37	0.01	-0.44	0.08	-0.85
9	-0.03	0.02	-0.05	0.01	-0.07	0.02	-0.07	0.04	-0.07	0.05	-0.08	0.16

**Table A7.** Values  $k_{i,j}$  of stiffness matrix  $\mathbf{k}$  expressed in MN/m, for  $n = 32$  and  $k_{\text{fou}} = 50, 100, 150, 200, 250$  MN/m and  $k_{\text{fou}}$ -rigid (elements  $k_{j,j}$  ( $i = j$ ) are given in bold).

$i$	$k_{\text{fou}}, \text{MN/m}$											
	50		100		150		200		250		Rigid	
	$k_{i,1}$	$k_{i,3}$	$k_{i,1}$	$k_{i,3}$	$k_{i,1}$	$k_{i,3}$	$k_{i,1}$	$k_{i,3}$	$k_{i,1}$	$k_{i,3}$	$k_{i,1}$	$k_{i,3}$
1	<b>29.79</b>		<b>47.57</b>		<b>59.61</b>		<b>68.32</b>		<b>75.46</b>		<b>122.72</b>	
	-8.74	-5.31	-15.32	-8.73	-20.08	-11.10	-23.66	-12.86	26.68	-14.33	-48.46	-24.84
2		-8.59		-14.84		-19.22		-22.44		-25.11		-43.04
	<b>31.61</b>	-7.75	<b>51.71</b>	-13.96	<b>65.87</b>	-18.57	<b>76.39</b>	-22.11	<b>85.24</b>	-25.13	<b>148.23</b>	-47.75
3		-5.79		-9.29		-11.61		-13.25		-14.59		-23.18
	-8.83	<b>33.15</b>	-15.81	<b>54.76</b>	-20.93	<b>70.16</b>	-24.80	<b>81.72</b>	-28.09	<b>91.50</b>	-52.03	<b>162.99</b>
4		0.00		0.00		0.00		0.00		0.00		0.00
	0.00	-7.75	0.00	-13.96	0.00	-18.57	0.00	-22.11	0.00	-25.13	0.00	-47.754
5		-1.75		-2.21		-2.45		-2.60		-2.71		-3.31
	-4.06	-5.31	-6.31	-8.73	-7.80	-11.10	-8.88	-12.86	-9.77	-14.33	-15.84	-24.843
6		-0.46		-0.19		0.04		0.22		0.37		1.46
	-2.11	-3.11	-2.90	-4.67	-3.38	-5.68	-3.71	-6.40	-3.97	-7.00	-5.66	-11.073
7		0.24		0.75		1.11		1.37		1.58		2.98
	-0.77	-1.48	-0.76	-1.87	-0.70	-2.06	-0.64	-2.17	-0.59	-2.26	-0.14	-2.729
8		0.00		0.00		0.00		0.00		0.00		0.00
	0.00	0.00	0.00	0.00	0.00	0.00	0.00	0.00	0.00	0.00	0.00	1.46
9		0.58		0.84		0.96		1.04		1.09		1.35
	0.54	0.36	1.06	0.94	1.41	1.37	1.66	1.69	1.86	1.96	3.27	0

**Table A8.** Values  $f_{\text{obj},i,j}$ , [-], of the matrix  $\mathbf{f}_{\text{obj}}$  of object displacement forms for  $n = 3, 4, 8$ ,  $k_{\text{fou}} = 50, 100, 150, 200, 250$  MN/m and  $k_{\text{fou}}$ -rigid (elements  $f_{\text{obj},j,j}$  ( $i = j$ ) are given in bold).

$n$	$f_{\text{obj},i,j}$	$k_{\text{fou}}, \text{MN/m}$					
		50	100	150	200	250	Rigid
3	$f_{\text{obj},1,1}$	<b>1</b>	<b>1</b>	<b>1</b>	<b>1</b>	<b>1</b>	<b>1</b>
	$f_{\text{obj},1,2}$	0	0	0	0	0	0
4	$f_{\text{obj},1,1}$	<b>0.952</b>	<b>0.973</b>	<b>0.981</b>	<b>0.985</b>	<b>0.988</b>	<b>0.998</b>
	$f_{\text{obj},2,1}$	0.076	0.059	0.052	0.049	0.046	0.038
	$f_{\text{obj},3,1}$	-0.073	-0.056	-0.05	-0.047	-0.045	-0.036

Table A8. Cont.

<i>n</i>	$f_{obj,i,j}$	$k_{fou}$ , MN/m					Rigid
		50	100	150	200	250	
8	$f_{obj,1,1}$	<b>0.761</b>	<b>0.844</b>	<b>0.882</b>	<b>0.905</b>	<b>0.92</b>	<b>0.988</b>
	$f_{obj,2,1}$	0.246	0.227	0.218	0.213	0.209	0.192
	$f_{obj,3,1}$	−0.026	−0.037	−0.04	−0.042	−0.043	−0.045
	$f_{obj,4,1}$	−0.024	−0.017	−0.015	−0.013	−0.012	−0.008
	$f_{obj,5,1}$	−0.002	0.003	0.004	0.005	0.005	0.006

Table A9. Values  $f_{obj,i,j}$  [-] of the matrix  $f_{obj}$  of object displacement forms for  $n = 16$ ,  $k_{fou} = 50, 100, 150, 200, 250$  MN/m and  $k_{fou}$ -rigid (elements  $f_{obj,i,i}$  ( $i = j$ ) are given in bold).

<i>i</i>	$k_{fou}$ , MN/m											
	50		100		150		200		250		Rigid	
	$f_{obj,i,1}$	$f_{obj,i,2}$	$f_{obj,i,1}$	$f_{obj,i,2}$	$f_{obj,i,1}$	$f_{obj,i,2}$	$f_{obj,i,1}$	$f_{obj,i,2}$	$f_{obj,i,1}$	$f_{obj,i,2}$	$f_{obj,i,1}$	$f_{obj,i,2}$
1	<b>0.555</b>	0.325	<b>0.667</b>	0.366	<b>0.730</b>	0.390	<b>0.771</b>	0.405	<b>0.802</b>	0.418	<b>0.966</b>	0.486
2	0.315	<b>0.484</b>	0.346	<b>0.599</b>	0.363	<b>0.667</b>	0.374	<b>0.714</b>	0.382	<b>0.750</b>	0.424	<b>0.954</b>
3	0.109	0.325	0.096	0.366	0.090	0.390	0.086	0.405	0.084	0.418	0.072	0.486
4	0.003	0.125	−0.012	0.122	−0.018	0.121	−0.022	0.121	−0.024	0.121	−0.036	0.122
5	−0.033	0.002	−0.036	−0.014	−0.036	−0.021	−0.036	−0.025	−0.036	−0.028	−0.035	−0.043
6	−0.019	−0.012	−0.017	−0.014	−0.016	−0.014	−0.016	−0.014	−0.015	−0.014	−0.013	−0.013
7	−0.010	−0.021	−0.006	−0.019	−0.005	−0.018	−0.004	−0.018	−0.003	−0.017	−0.001	−0.017
8	0.000	0.000	0.000	0.004	0.000	0.006	0.000	0.007	0.000	0.008	−0.001	0.012
9	0.001	−0.001	0.001	0.000	0.001	0.000	0.001	−0.001	0.001	−0.001	0.001	−0.002

Table A10. Values  $f_{obj,i,j}$  [-] of the matrix  $f_{obj}$  of object displacement forms for  $n = 32$ ,  $k_{fou} = 50, 100, 150, 200, 250$  MN/m and  $k_{fou}$ -rigid (elements  $f_{obj,i,i}$  ( $i = j$ ) are given in bold).

<i>i</i>	$k_{fou}$ , MN/m											
	50		100		150		200		250		Rigid	
	$f_{obj,i,1}$		$f_{obj,i,1}$		$f_{obj,i,1}$		$f_{obj,i,1}$		$f_{obj,i,1}$		$f_{obj,i,1}$	
	$f_{obj,i,2}$	$f_{obj,i,3}$	$f_{obj,i,2}$	$f_{obj,i,3}$	$f_{obj,i,2}$	$f_{obj,i,3}$	$f_{obj,i,2}$	$f_{obj,i,3}$	$f_{obj,i,2}$	$f_{obj,i,3}$	$f_{obj,i,2}$	$f_{obj,i,3}$
1	<b>0.387</b>		<b>0.497</b>		<b>0.569</b>		<b>0.661</b>		<b>0.661</b>		<b>0.930</b>	
	0.294	0.179	0.363	0.207	0.409	0.226	0.442	0.240	0.470	0.252	0.664	0.654
2	0.290		0.352		0.391		0.442		0.442		0.589	
	<b>0.350</b>	0.261	<b>0.453</b>	0.331	<b>0.523</b>	0.378	<b>0.575</b>	0.413	<b>0.617</b>	0.443	<b>0.916</b>	0.654
3	0.195		0.220		0.236		0.257		0.257		0.317	
	0.297	<b>0.318</b>	0.374	<b>0.421</b>	0.426	<b>0.492</b>	0.464	<b>0.545</b>	0.495	<b>0.617</b>	0.712	<b>0.907</b>
4	0.000		0.000		0.000		0.000		0.000		0.000	
	0.000	0.261	0.000	0.331	0.000	0.378	0.000	0.413	0.000	0.443	0.000	0.654
5	0.059		0.052		0.050		0.048		0.048		0.045	
	0.137	0.179	0.149	0.207	0.159	0.226	0.166	0.240	0.172	0.252	0.217	0.340
6	0.016		0.005		−0.001		−0.007		−0.007		−0.020	
	0.071	0.105	0.069	0.111	0.069	0.116	0.069	0.120	0.070	0.123	0.078	0.152
7	−0.008		−0.018		−0.023		−0.028		−0.028		−0.041	
	0.026	0.050	0.018	0.044	0.014	0.042	0.012	0.041	0.010	0.040	0.002	0.037
8	0.000		0.000		0.000		0.000		0.000		0.000	
	0.000	0.000	0.000	0.000	0.000	0.000	0.000	0.000	0.000	0.000	0.000	0.000
9	−0.020		−0.020		−0.020		−0.019		−0.019		−0.019	
	−0.018	−0.012	−0.025	−0.022	−0.029	−0.028	−0.031	−0.032	−0.033	−0.035	−0.045	−0.054

**Table A11.** Values  $f_{fou,i,j}$  [-] of the matrix  $f_{fou}$  of support displacement forms for  $n = 3, 4, 8$ ,  $k_{fou} = 50, 100, 150, 200, 250$  MN/m and  $k_{fou}$ -rigid (elements  $f_{fou,j,j}$  ( $i = j$ ) are given in bold).

$n$	$f_{fou,i,j}$	$k_{fou}$ , MN/m					Rigid
		50	100	150	200	250	
3	$f_{fou,1,1}$	<b>0</b>	<b>0</b>	<b>0</b>	<b>0</b>	<b>0</b>	<b>0</b>
	$f_{fou,1,2}$	0	0	0	0	0	0
4	$f_{fou,1,1}$	<b>-0.047</b>	<b>-0.026</b>	<b>-0.018</b>	<b>-0.014</b>	<b>-0.011</b>	<b>0</b>
	$f_{fou,2,1}$	0.045	0.025	0.017	0.013	0.010	0
	$f_{fou,3,1}$	-0.043	-0.024	-0.016	-0.013	-0.010	0
8	$f_{fou,1,1}$	<b>-0.232</b>	<b>-0.147</b>	<b>-0.108</b>	<b>-0.086</b>	<b>-0.070</b>	<b>0</b>
	$f_{fou,2,1}$	0.146	0.096	0.072	0.057	0.047	0
	$f_{fou,3,1}$	-0.015	-0.016	-0.013	-0.011	-0.010	0
	$f_{fou,4,1}$	-0.014	-0.007	-0.005	-0.004	-0.003	0
	$f_{fou,5,1}$	-0.001	0.001	0.001	-0.004	0.001	0

**Table A12.** Values  $f_{fou,i,j}$  [-] of the matrix  $f_{fou}$  of support displacement forms for  $n = 16$ ,  $k_{fou} = 50, 100, 150, 200, 250$  MN/m and  $k_{fou}$ -rigid (elements  $f_{fou,j,j}$  ( $i = j$ ) are given in bold).

$i$	$k_{fou}$ , MN/m											
	50		100		150		200		250		Rigid	
	$f_{fou,i,1}$	$f_{fou,i,2}$	$f_{fou,i,1}$	$f_{fou,i,2}$	$f_{fou,i,1}$	$f_{fou,i,2}$	$f_{fou,i,1}$	$f_{fou,i,2}$	$f_{fou,i,1}$	$f_{fou,i,2}$	$f_{fou,i,1}$	$f_{fou,i,2}$
1	<b>-0.433</b>	0.193	<b>-0.315</b>	0.154	<b>-0.248</b>	0.128	<b>-0.205</b>	0.108	<b>-0.173</b>	0.093	<b>0</b>	0
2	0.187	<b>-0.501</b>	0.146	<b>-0.380</b>	0.119	<b>-0.306</b>	0.100	<b>-0.257</b>	0.085	<b>-0.219</b>	0	<b>0</b>
3	0.065	0.193	0.040	0.154	0.029	0.128	0.023	0.108	0.019	0.093	0	0
4	0.002	0.074	-0.005	0.051	-0.006	0.040	-0.006	0.032	-0.005	0.027	0	0
5	-0.020	0.001	-0.015	-0.006	-0.012	-0.007	-0.010	-0.007	-0.008	-0.006	0	0
6	-0.012	-0.007	-0.007	-0.006	-0.005	-0.005	-0.004	-0.004	-0.003	-0.003	0	0
7	-0.006	-0.012	-0.003	-0.008	-0.002	-0.006	-0.001	-0.005	-0.001	-0.004	0	0
8	0.000	0.000	0.000	0.002	0.000	0.002	0.000	0.002	0.000	0.002	0	0
9	0.001	0.000	0.001	0.000	0.000	0.000	0.000	0.000	0.000	0.000	0	0

**Table A13.** Values  $f_{fou,i,j}$  [-] of the matrix  $f_{fou}$  of support displacement forms for  $n = 32$ ,  $k_{fou} = 50, 100, 150, 200, 250$  MN/m and  $k_{fou}$ -rigid (elements  $f_{fou,j,j}$  ( $i = j$ ) are given in bold).

$i$	$k_{fou}$ , MN/m											
	50		100		150		200		250		Rigid	
	$f_{fou,i,1}$	$f_{fou,i,3}$	$f_{fou,i,1}$	$f_{fou,i,3}$	$f_{fou,i,1}$	$f_{fou,i,3}$	$f_{fou,i,1}$	$f_{fou,i,3}$	$f_{fou,i,1}$	$f_{fou,i,3}$	$f_{fou,i,1}$	$f_{fou,i,3}$
1	<b>-0.596</b>		<b>-0.476</b>		<b>-0.397</b>		<b>-0.342</b>		<b>-0.296</b>		<b>0</b>	
	0.175	0.106	0.153	0.088	0.134	0.074	0.118	0.065	0.105	0.057	0	0
2	0.172		0.148		0.128		0.112		0.098		0	
	<b>-0.632</b>	0.155	<b>-0.517</b>	0.140	<b>-0.439</b>	0.124	<b>-0.382</b>	0.111	<b>-0.334</b>	0.099	<b>0</b>	0
3	0.116		0.093		0.077		0.066		0.057		0	
	0.177	<b>-0.663</b>	0.158	<b>-0.548</b>	0.140	<b>-0.468</b>	0.124	<b>-0.409</b>	0.110	<b>-0.359</b>	0	<b>0</b>
4	0.000		0.000		0.000		0.000		0.000		0	
	0.000	0.155	0.000	0.140	0.000	0.124	0.000	0.111	0.000	0.099	0	0
5	0.035		0.022		0.016		0.013		0.011		0	
	0.081	0.106	0.063	0.087	0.052	0.074	0.044	0.064	0.038	0.056	0	0
6	0.009		0.002		0.000		-0.001		-0.001		0	
	0.042	0.062	0.029	0.047	0.023	0.038	0.019	0.032	0.016	0.027	0	0
7	-0.005		-0.008		-0.007		-0.007		-0.006		0	
	0.015	0.030	0.008	0.019	0.005	0.014	0.003	0.011	0.002	0.009	0	0
8	0.000		0.000		0.000		0.000		0.000		0	
	0.000	0.000	0.000	0.000	0.000	0.000	0.000	0.000	0.000	0.000	0	0
9	-0.012		-0.008		-0.006		-0.005		-0.004		0	
	-0.011	-0.007	-0.011	-0.009	-0.009	-0.009	-0.008	-0.008	-0.007	-0.008	0	0

**Table A14.** Work done by the jacks during the forced piston extension in all the jacks by  $u_{\text{ext}} = 1$  mm and mean displacement of the object  $u_{\text{obj-mean}}$  for  $n = 3, 4, 8, 16$  and  $32$ ,  $k_{\text{fou}} = 50, 100, 150, 200, 250$  MN/m and  $k_{\text{fou-rigid}}$ .

$n$	$k_{\text{fou}}$ , MN/m	50	100	150	200	250	Rigid
3	W, kJ	1.347	1.347	1.347	1.347	1.347	1.347
	$u_{\text{obj-mean}}$ , mm	1	1	1	1	1	1
	$W/u_{\text{obj-mean}}$ kJ/mm	1.347	1.347	1.347	1.347	1.347	1.347
4	W, kJ	1.347	1.347	1.347	1.347	1.347	1.347
	$u_{\text{obj-mean}}$ , mm	1.031	1.035	1.035	1.036	1.035	1.038
	$W/u_{\text{obj-mean}}$ kJ/mm	1.306	1.301	1.301	1.300	1.301	1.297
8	W, kJ	1.347	1.347	1.347	1.347	1.347	1.347
	$u_{\text{obj-mean}}$ , mm	1.151	1.193	1.212	1.226	1.233	1.272
	$W/u_{\text{obj-mean}}$ kJ/mm	1.170	1.129	1.111	1.098	1.092	1.059
16	W, kJ	1.366	1.362	1.359	1.357	1.356	1.350
	$u_{\text{obj-mean}}$ , mm	1.307	1.461	1.547	1.606	1.657	1.923
	$W/u_{\text{obj-mean}}$ kJ/mm	1.045	0.932	0.879	0.845	0.818	0.702
32	W, kJ	1.373	1.387	1.396	1.403	1.409	1.448
	$u_{\text{obj-mean}}$ , mm	1.414	1.677	1.857	1.995	2.106	2.911
	$W/u_{\text{obj-mean}}$ kJ/mm	0.971	0.827	0.752	0.703	0.669	0.497

**Table A15.** Force  $Q_g$ , in the jacks depending on the  $n$  number of the jacks and stiffness  $k_{\text{fou}}$  of jack supports.

$n$	$Q_{g,i}$	$k_{\text{fou}}$ , MN/m					
		50	100	150	200	250	rigid
3	$Q_{g,1}$ , kN	431.30	431.30	431.30	431.30	431.30	431.30
	$Q_{g,2}$ , kN	457.80	457.80	457.80	457.80	457.80	457.80
4	$Q_{g,1}$ , kN	336.72	336.72	336.72	336.72	336.72	336.72
8	$Q_{g,1}$ , kN	168.35	168.35	168.35	168.35	168.35	168.35
16	$Q_{g,1}$ , kN	66.65	60.05	56.59	54.46	52.90	45.50
	$Q_{g,2}$ , kN	101.69	108.28	111.74	113.86	115.43	122.82
32	$Q_{g,1}$ , kN	21.33	13.49	9.37	6.83	4.96	−3.89
	$Q_{g,2}$ , kN	46.21	47.83	48.69	49.22	49.62	51.51
	$Q_{g,3}$ , kN	54.60	59.27	61.70	63.19	64.28	69.42

## References

- Kalantari, B. Foundations on Collapsible Soils: A Review. In *Proceedings of the Institution of Civil Engineers—Forensic Engineering*; Thomas Telford Ltd.: London, UK, 2013; Volume 166, pp. 57–63. [\[CrossRef\]](#)
- Puzrin, A.M.; Alonso, E.E.; Pinyol, N.M. Bearing Capacity Failure: Transcona Grain Elevator, Canada. In *Geomechanics of Failures*; Springer: Dordrecht, The Netherlands, 2010; pp. 67–84, ISBN 978-90-481-3530-1.
- Baracous, A. The Foundation Failure of the Transcona Grain Elevator. *Eng. J.* **1957**, *40*, 973–977.
- Macchi, G. Stabilization of the Leaning Tower of Pisa. In *Proceedings of the Structures Congress 2005*, New York, NY, USA, 18 April 2005; American Society of Civil Engineers: Reston, VA, USA, 2005; pp. 1–11.
- Gromysz, K. Revitalisation of a Vertically Deflected Historical 16th Century Bell Tower. *IOP Conf. Ser. Mater. Sci. Eng.* **2019**, *471*, 052025. [\[CrossRef\]](#)
- Li, S.; Song, T.; Milani, G.; Abruzzese, D.; Yuan, J. An Iterative Rectification Procedure Analysis for Historical Timber Frames: Application to a Cultural Heritage Chinese Pavilion. *Eng. Struct.* **2021**, *227*, 111415. [\[CrossRef\]](#)
- Ovando-Shelley, E.; Santoyo, E. Underexcavation for Leveling Buildings in Mexico City: Case of the Metropolitan Cathedral and the Sagrario Church. *J. Arch. Eng.* **2001**, *7*, 61–70. [\[CrossRef\]](#)
- Kijanka, M.; Kowalska, M. Inclined Buildings—Some Reasons and Solutions. *IOP Conf. Ser. Mater. Sci. Eng.* **2017**, *245*, 022052. [\[CrossRef\]](#)

9. Ragite, N.C. Outrigger Structural System in High Rise Building to Control Deflection: A Review. *IJRASET* **2019**, *7*, 3490–3493. [[CrossRef](#)]
10. Smith, R. Deflection Limits in Tall Buildings—Are They Useful? In Proceedings of the Structures Congress 2011, Las Vegas, NV, USA, 13 April 2011; American Society of Civil Engineers: Reston, VA, USA, 2011; pp. 515–527.
11. Baghban Golpasand, M.-R.; Do, N.A.; Dias, D. Impact of Pre-Existent Qanats on Ground Settlements Due to Mechanized Tunneling. *Transp. Geotech.* **2019**, *21*, 100262. [[CrossRef](#)]
12. Orwat, J. Causes Analysis of Occurrence of the Terrain Surface Discontinuous Deformations of a Linear Type. *J. Phys. Conf. Ser.* **2020**, *1426*, 012016. [[CrossRef](#)]
13. Whittaker, B.N.; Reddish, D.J. *Subsidence. Occurrence, Prediction and Control*; Developments in Geotechnical Engineering; Elsevier: Amsterdam, The Netherlands; Oxford, UK; New York, NY, USA; Tokyo, Japan, 1989; ISBN 0-444-87274-4.
14. Piwowarski, W. Analysis of Rock Mass Destruction Processes with Different Activity Diagrams. *Acta Geodyn. Geomater.* **2017**, *1*, 83–92. [[CrossRef](#)]
15. Orwat, J. Mining Terrain Curvatures Approximation Using the Polynomials and a Subsidence Trough Profile Fragmentation. *J. Phys. Conf. Ser.* **2021**, *1781*, 012014. [[CrossRef](#)]
16. Orwat, J.; Gromysz, K. Occurrence Consequences of Mining Terrain Surface Discontinuous Linear Deformations in a Residential Building. *J. Phys. Conf. Ser.* **2021**, *1781*, 012013. [[CrossRef](#)]
17. Li, Z.; Luo, Z.; Wang, Q.; Du, J.; Lu, W.; Ning, D. A Three-Dimensional Fluid-Solid Model, Coupling High-Rise Building Load and Groundwater Abstraction, for Prediction of Regional Land Subsidence. *Hydrogeol. J.* **2019**, *27*, 1515–1526. [[CrossRef](#)]
18. Milani, G.; Shehu, R.; Valente, M. Seismic Assessment of Masonry Towers by Means of Nonlinear Static Procedures. *Procedia Eng.* **2017**, *199*, 266–271. [[CrossRef](#)]
19. Bońkowski, P.A.; Zembaty, Z.; Minch, M.Y. Seismic Effects on Leaning Slender Structures and Tall Buildings. *Eng. Struct.* **2019**, *198*, 109518. [[CrossRef](#)]
20. Gagliardo, R.; Portioli, F.P.A.; Cascini, L.; Landolfo, R.; Lourenço, P.B. A Rigid Block Model with No-Tension Elastic Contacts for Displacement-Based Assessment of Historic Masonry Structures Subjected to Settlements. *Eng. Struct.* **2021**, *229*, 111609. [[CrossRef](#)]
21. Strzałkowski, P. Some Remarks on Impact of Mining Based on an Example of Building Deformation and Damage Caused by Mining in Conditions of Upper Silesian Coal Basin. *Pure Appl. Geophys.* **2019**, *176*, 2595–2605. [[CrossRef](#)]
22. Ren, C.; Yan, B. Experimental Research of the Influence of Differential Settlement on the Upper Frame Structures. In Proceedings of the 3rd International Conference on Mechanical Engineering and Intelligent Systems (ICMEIS 2015), Yinchuan, China, 15–16 August 2015; Atlantis Press: Amsterdam, The Netherlands, 2015.
23. Zhang, B.; Chen, F.; Wang, Q.; Lin, L. Analytical Model of Buried Beams on a Tensionless Foundation Subjected to Differential Settlement. *Appl. Math. Model.* **2020**, *87*, 269–286. [[CrossRef](#)]
24. Al' Malul, R.; Gadzhuntsev, M. The Reliability of Multistory Buildings with the Effect of Non-Uniform Settlements of Foundation. *E3S Web Conf.* **2018**, *33*, 02040. [[CrossRef](#)]
25. Peck, R.B.; Bryant, F.G. The Bearing-Capacity Failure of the Transcona Elevator. *Géotechnique* **1953**, *3*, 201–208. [[CrossRef](#)]
26. Yin, H.P.; Li, C.L.; Xie, Z.Y. Analysis on Deviation Rectification and Reinforcement of Buildings. *AMR* **2011**, *255–260*, 59–64. [[CrossRef](#)]
27. Sternik, K.; Blejarski, T. Application of Micropiles to the Stabilization of a Deflected Old Tenement House. In Proceedings of the 12th International Workshop on Micropiles, Kraków, Poland, 11–14 June 2014; pp. 1–12.
28. Gromysz, K.; Szoblik, Ł.; Cyrulik, E.; Tanistra-Różanowska, A.; Drabczyk, Z.; Jancia, S. Analysis of Stabilisation Method of Gable Walls of a Barrack Located at the Section BI of the Former KL Auschwitz II-Birkenau. *MATEC Web Conf.* **2019**, *284*, 08004. [[CrossRef](#)]
29. Gromysz, K.; Szoblik, Ł.; Cyrulik, E.; Tanistra-Rozanowska, A.; Drabczyk, Z.; Jancia, S. Rectification of Walls of the Historical Brick Barrack on the Site of the Former German Nazi Concentration and Extermination Camp KL Auschwitz—Birkenau. *IOP Conf. Ser. Mater. Sci. Eng.* **2019**, *603*, 042070. [[CrossRef](#)]
30. Gromysz, K. Analysis of the Effect of Load Application Eccentricity on the Stiffness of Supports Consisting of Stack of Elements. *MATEC Web Conf.* **2019**, *262*, 10005. [[CrossRef](#)]
31. Yang, X. Application of Comprehensive Rectification Method in Rectification of Buildings. *E3S Web Conf.* **2020**, *165*, 04004. [[CrossRef](#)]
32. Yang, H.T.; Zhou, L. The Application on Stress Relief Method in Deviation Correction of Buildings. *AMM* **2013**, *405–408*, 441–444. [[CrossRef](#)]
33. Yue, Q.; Zhang, X. Experimental Study on the Stress Distribution and Failure Mode of the Holes for Underexcavation in Building Rectification. In Proceedings of the Geo-Congress 2020, Minneapolis, MN, USA, 21 February 2020; American Society of Civil Engineers: Reston, VA, USA, 2020; pp. 269–278.
34. Gromysz, K. Examples of Even Lifting of Structural Elements of Existing Buildings. *IOP Conf. Ser. Mater. Sci. Eng.* **2020**, *960*, 032050. [[CrossRef](#)]
35. Gromysz, K. In Situ Experimental Study on the Active Support Used for Building Rectification. *Materials* **2020**, *13*, 2015. [[CrossRef](#)]
36. Gromysz, K.; Orwat, J. Removal of Deflection and Reconstruction of Foundations of the Historic Museum Building. *IOP Conf. Ser. Mater. Sci. Eng.* **2020**, *960*, 032051. [[CrossRef](#)]